A Preliminary Investigation of Fish Distributions near an In-Stream Tidal Turbine in Minas Passage, Bay of Fundy

G.D. Melvin and N.A. Cochrane

Fisheries and Oceans Canada
Biological Station
531 Brandy Cove Road
St. Andrews, NB
E5B 2L9

2012

Canadian Technical Report of Fisheries and Aquatic Sciences 3006

Fisheries and Oceans Canada
Pêches et Océans Canada

Canada

Canadian Technical Report of Fisheries and Aquatic Sciences

Technical reports contain scientific and technical information that contributes to existing knowledge but which is not normally appropriate for primary literature. Technical reports are directed primarily toward a worldwide audience and have an international distribution. No restriction is placed on subject matter and the series reflects the broad interests and policies of Fisheries and Oceans Canada, namely, fisheries and aquatic sciences.

Technical reports may be cited as full publications. The correct citation appears above the abstract of each report. Each report is abstracted in the data base *Aquatic Sciences and Fisheries Abstracts*.

Technical reports are produced regionally but are numbered nationally. Requests for individual reports will be filled by the issuing establishment listed on the front cover and title page.

Numbers 1-456 in this series were issued as Technical Reports of the Fisheries Research Board of Canada. Numbers 457-714 were issued as Department of the Environment, Fisheries and Marine Service, Research and Development Directorate Technical Reports. Numbers 715-924 were issued as Department of Fisheries and Environment, Fisheries and Marine Service Technical Reports. The current series name was changed with report number 925.

Rapport technique canadien des sciences halieutiques et aquatiques

Les rapports techniques contiennent des renseignements scientifiques et techniques qui constituent une contribution aux connaissances actuelles, mais qui ne sont pas normalement appropriés pour la publication dans un journal scientifique. Les rapports techniques sont destinés essentiellement à un public international et ils sont distribués à cet échelon. II n'y a aucune restriction quant au sujet; de fait, la série reflète la vaste gamme des intérêts et des politiques de Pêches et Océans Canada, c'est-à-dire les sciences halieutiques et aquatiques.

Les rapports techniques peuvent être cités comme des publications à part entière. Le titre exact figure au-dessus du résumé de chaque rapport. Les rapports techniques sont résumés dans la base de données *Résumés des sciences aquatiques et halieutiques.*

Les rapports techniques sont produits à l'échelon régional, mais numérotés à l'échelon national. Les demandes de rapports seront satisfaites par l'établissement auteur dont le nom figure sur la couverture et la page du titre.

Les numéros 1 à 456 de cette série ont été publiés à titre de Rapports techniques de l'Office des recherches sur les pêcheries du Canada. Les numéros 457 à 714 sont parus à titre de Rapports techniques de la Direction générale de la recherche et du développement, Service des pêches et de la mer, ministère de l'Environnement. Les numéros 715 à 924 ont été publiés à titre de Rapports techniques du Service des pêches et de la mer, ministère des Pêches et de l'Environnement. Le nom actuel de la série a été établi lors de la parution du numéro 925.

Canadian Technical Report of
Fisheries and Aquatic Sciences 3006

2012

A PRELIMINARY INVESTIGATION OF FISH DISTRIBUTIONS NEAR AN IN-STREAM TIDAL TURBINE IN MINAS PASSAGE, BAY OF FUNDY

by

Gary D. Melvin[1] and Norman A. Cochrane[2]

[1]Department of Fisheries & Oceans
St. Andrews Biological Station (SABS)
531 Brandy Cove Road
St. Andrews, New Brunswick E5B 2L9

[2]Department of Fisheries & Oceans
Bedford Institute of Oceanography (BIO
1 Challenger Drive, PO Box 1006
Dartmouth, Nova Scotia B2Y 4A2

This is the **three hundred and eighty second** Technical Report
of the Biological Station, St. Andrews, NB

Cat. No. Fs 97-6/2840E-PDF ISSN 1488-5379 (online version)

Correct citation for this publication:

Melvin, Gary D. and Cochrane, Norman A. 2012. A Preliminary Investigation of Fish Distributions Near an In-Stream Tidal Turbine in Minas Passage, Bay of Fundy. Can. Tech. Rep. Fish. Aquat. Sci. 3006: vi + 43 p.

TABLE OF CONTENTS

LIST OF FIGURES

ABSTRACT

Melvin, Gary D. and Cochrane, Norman A. 2012. A Preliminary Investigation of Fish Distributions near an In-Stream Tidal Turbine in Minas Passage, Bay of Fundy. Can.Tech. Rep. Fish. Aquat. Sci. 3006: vi + 43 p.

The inner the Bay of Fundy, has been identified as one of the primary locations in eastern Canada for the installation of tidal in-stream energy conversion (TISEC) devices. Unfortunately, the physical characteristics of the passage, water clarity, and tidal currents/flow make the use of a suite of conventional monitoring tools, including video and bottom trawls, impractical. This study evaluates the capability in terms of detection and range of conventional single (Simrad EK60 split beam) and multi-beam (Kongsberg-Mesotech MS 2000) surface-mounted active sonars to monitor the distribution, abundance, and behaviour of fish-like targets in Minas Passage and in the vicinity of a deployed tidal turbine. A series of survey transects, including one passing directly over the OpenHydro turbine, were continuously run at the FORCE test site just east of Black Rock over a period of approximately 8 hours.

Tidal and wind generated surface backscatter noise during peak flow periods on occasion extended from the surface to bottom, but was usually limited to <15 m from the surface. Acoustic backscatter levels and fish target counts were examined from both systems with respect to their number, abundance (density), and position in the water column throughout a single tidal phase. Target detection in and around the bubble clouds was problematic and somewhat subjective. Acoustic targets were observed at two backscatter-defined modal depths between 10 - 20 m and 30 - 40 m. The modal depths varied depending upon the tidal phase. Occasionally a third mode occurred in the deeper water portions of the transects. The study concluded that conventional surface-based acoustic technology can be used to detect fish distribution and abundance throughout the water column below the surface backscatter noise. There are, however, some concerns regarding the detection of individual fish in or near the surface waters. Observations near the actual turbine structure will also be difficult using surface platforms.

RÉSUMÉ

Melvin, Gary D. et Cochrane, Norman A. 2012. Étude préliminaire de la répartition du poisson près d'une turbine marémotrice en eau vive dans le passage Minas de la baie de Fundy. Can.Tech. Rep. Fish. Aquat. Sci. 3006 : vi + 43 pages.

L'intérieur de la baie de Fundy a été désigné comme l'un des emplacements principaux dans l'Est du Canada pour installer des convertisseurs d'énergie marémotrice (TISEC). Malheureusement, les caractéristiques physiques du passage, soit la limpidité de l'eau, les courants de marée et le débit, rendent impossible l'utilisation d'un ensemble d'outils de surveillance classiques, y compris les vidéos et le chalutage par le fond. Cette étude évalue la capacité en matière de détection et d'éventail de sonar classique actif monté en surface à faisceau unique (Simrad EK60 à faisceau divisé) et à faisceaux multiples (Kongsberg-Mesotech MS 2000), pour ce qui est de la surveillance de la répartition, de l'abondance et du comportement des poissons ciblés dans le passage Minas et à proximité d'une turbine marémotrice en exploitation. Une série de relevés de transect, dont une passant directement au-dessus de la turbine OpenHydro, fonctionnait de façon continue au site d'essai du centre de recherche FORCE, tout juste à l'est de Black Rock, au cours d'une période d'environ huit heures.

Le bruit de rétrodiffusion en surface généré par le vent et les marées au cours des périodes de débit maximal s'élevait parfois de la surface au fond, mais était habituellement limité à une profondeur inférieure à 15 mètres de la surface. Les niveaux acoustiques de rétrodiffusion et les dénombrements des poissons ciblés ont fait l'objet d'un examen des deux systèmes quant à leur numéro, à leur abondance (densité) et quant à la position de la colonne d'eau au cours d'une seule phase de la marée. La détection de la cible au sein et autour des nuages de bulles s'est avérée problématique et quelque peu subjective. Les cibles acoustiques ont été étudiées à deux profondeurs modales définies par la rétrodiffusion, soit entre 10 mètres et 20 mètres de profondeur et entre 30 mètres et 40 mètres de profondeur. Les profondeurs modales varient en fonction de la phase de la marée. À l'occasion, un troisième modèle est étudié dans les parties des transects où l'eau est plus profonde. L'étude a permis de conclure que la technologie acoustique de surface classique peut être utilisée pour détecter la répartition et l'abondance des poissons dans la colonne d'eau d'une fréquence inférieure au bruit de rétrodiffusion en surface. Cependant, la détection des poissons dans les eaux superficielles ou près de ces dernières soulève certaines préoccupations. Les observations à l'aide des plateformes de surface près de la turbine s'avéreront également difficiles.

INTRODUCTION

GENERAL

The inner the Bay of Fundy, has been identified as one of the key locations for the installation of tidal in-stream energy conversion (TISEC) devices. Based on a CHC technical report summarizing 3-D modeling and assessment of tidal current energy resources (Durand et al. 2008), the potential power generation capacity in Minas Passage exceeds all other areas in the Bay of Fundy. The Passage is also home to a number of fish, marine mammals, and invertebrate species. Currently there are in excess of 50 species of fish and invertebrates (commercial and non-commercial) inhabiting or passing through Minas Passage on an annual basis. Knowledge of when these species are present in the Passage, how these species are distributed vertically and horizontally in the water column, whether they are long term or transient inhabitants, and their reaction/behaviour to a turbine is critical to our understanding of the risks associated with the safe deployment of tidal turbine devices and the large scale development of TISEC-based tidal power.

Emplacement of Bay of Fundy TISEC technology has taken a sequential approach beginning with the identification of potential development sites, establishment of a test site in Minas Passage, and the initial test deployment of a turbine unit. At the time of this report the Fundy Ocean Research Center for Energy (FORCE) turbine evaluation site just west of Black Rock, Nova Scotia was the only location with an active device deployed on the east coast of Canada. The OpenHydro turbine was installed on the 12th November 2009 but the operational status of the turbine was uncertain for a large portion of its deployment due to the failure of the acoustic telemetry system soon after the unit was put in the water. A camera survey in March 2010, widely reported in the media, indicated that two turbine blades were missing. The turbine was removed on the 16th December 2010, at which time all turbine blades were missing, so the actual operational period of the turbine is unknown.

The physical characteristics of the passage, water clarity, and tidal currents/flow preclude use of a conventional suite of biological monitoring tools, including video and bottom trawls, making use of acoustic sensing techniques advantageous. An earlier pre-installation trial acoustic survey in the same general area (Melvin et al. 2009) disclosed high levels of acoustic backscatter in the upper half of the water column. This appears to arise from the tide rip associated bubble cloud aeration extending westward from the vicinity of Black Rock. While bubble cloud backscatter can, and did, obscure biological targets in the upper water column there was no detectable associated attenuation of acoustic backscatter echoes from the lower portions of the water column. This means that targets outside the multiple bubble clouds can be detected and quantified acoustically.

The purpose of this present study was to evaluate the capability (detection and range) of conventional single and multi-beam sonars to monitor the distribution, abundance, and behaviour of fish-like targets in the Passage and in the vicinity of an actual turbine using surface-mounted active acoustic systems.

METHODS

STUDY AREA

Minas Passage, located in the inner Bay of Fundy, is a relatively narrow passage, approximately 12 km long and 5 km wide, that allows the flow of tidal waters into and out of Minas Basin (Fig. 1). The passage is characterized by strong, predominately lunar semi-diurnal (M_2) period tidal currents ranging from 6 - 8 knots (3.0 - 4.1 m/s) during maximum flow with average tidal amplitude of 10 m and peaks of greater than 13.0 m (Tides & Currents Software, Version 1.05). Water depths in the passage can exceed 135 m, but at the test turbine site range from 28 – 41 m depending upon the tide. Detailed physical characteristics of the passage are available in several published reports (Durand et al. 2008, AECOM 2009).

SURVEY PLATFORM/INSTRUMENTATION

The *Fundy Spray* (Fig. 2), a 15.4 m, 38 gross ton small passenger vessel, was used to survey the existing turbine site and nearby area in Minas Passage. Two active acoustic systems were deployed from the vessel for surveying; (i) a split-beam echo-sounder (Simrad EK60) and (ii) a 2-D multi-beam sonar (Kongsberg-Mesotech MS 2000). Both the EK60 (120 kHz, 7° beam angle) and the MS 2000 sonar (200 kHz, 180° fan swath, beam angle approx. 2.5^0 fan x 1.5^o) were pole-mounted (Fig. 3) and deployed at about 2 m depth from the starboard side of the vessel. This enabled delineation of a port-starboard fan swath beneath the survey vessel. The set-up was similar to that utilized on the earlier trial survey (Melvin et al. 2009). A shipboard differential GPS unit provided NEMA 083 serial data streams for GPS position to the EK60 and the MS 2000. Time was extracted from the computer clock. System-specific software was used for data logging; Simrad ER60 for the EK60 echo-sounder and Simrad MS 2000 Version 1.4.2 for the multi-beam sonar. The ping rate was set at 1.0/s for the SM2000 and 1.01 for the EK60 to minimize interference.

SURVEY

The survey goal was to monitor fish distributions in the vicinity of the turbine over a complete tidal cycle using acoustic technology deployed from a surface vessel. On 16 Sept. 2010 just over 6 hours of simultaneous 120 kHz split-beam and 200 kHz multi-beam data were collected near the Minas Passage turbine site. Upon reaching the test site the transducers were lowered to slightly below hull depth, fixed into position, and the

acoustics systems activated. An initial survey objective was to verify the exact position of the turbine relative to the co-ordinates (41° 21.897' N 64° 25.5762' W) provided by the developer. Data collection and the search for the turbine began on the 16th September 2010 at 12:16 GMT, about 2 hours past local high tide, and ended at 18:35 GMT, almost exactly 2 hours past local low tide - earlier than planned due to high winds and deteriorating seas (Fig. 4).

Once the turbine was located and its position verified by sonar, several passes were made over the device to determine the best approach direction given the system's orientation, tidal currents, and weather conditions (Fig. 5). Thereafter, a series of 7 transects were established approximately 100 m apart, 3 north and 3 south of a predominately east-west line that passed over the turbine (Fig. 1). The transects, which varied in length from 900 m to 1400 m, were surveyed sequentially and continuously until about 18:30 GMT when the vessel undertook several final passes over the turbine before heading to port/shelter. Additional acoustic data more remote from the turbine site were collected on the subsequent transit to Parrsboro. All data acquisition ended at 19:03 GMT. The EK60 system settings are presented in Table 1. Table 2 summarizes the location, time, tidal phase, and transect length. Table 3 summarizes the backscatter for each transect occupied throughout the day. Although the duration of true slack water in Minas Passage is very short, one hour before and after low tide (16:32 GMT) was considered slack tide for this report and the subsequent analyzes. Overall, data from 25 individual transects were collected with both the EK60 scientific echo-sounder and the MS 2000 multi-beam sonar (Fig. 6). All data were checked for completeness and archived on DVD prior to analysis.

ANALYSIS

Data Handling and Initial Processing

General

Data handling and initial processing of information from the two acoustic systems differed significantly. Both the EK60 and the MS 2000 collect relatively large volumes of data that must be scrutinized and edited to identify fish and non-fish targets prior to quantitative analysis. For the EK60 a commercial editing and analytical software package, Echoview Version 4.9 by Myriax, was used for all data analysis. Calibration parameters characteristic of the system and the environment were checked and updated if necessary (Table 1). Similar survey-oriented software was not available for analyzing the MS 2000 data and the analyses was conducted using analytical tools developed by the authors.

The split-beam and multi-beam systems provide complementary information that greatly improves the identification of fish-like targets from background noise in the editing phase of the analysis. The MS 2000 multi-beam's 180^0 beam fan samples a much larger water volume than the narrow 7^0 vertical beam of the EK60, potentially permitting a superior statistical description of, especially, shallow depth fish distributions and sparsely

distributed fish schools and aggregations. The EK60, in contrast, is an inherently more sensitive system which yields higher signal-to-noise ratio information on weakly scattering fish in the deeper portions of the water column. The EK60 is specifically designed for accurate fisheries quantification with standardized calibration protocols and widely accepted commercial analytical software. In contrast, the MS 2000 remains largely an experimental system for fisheries applications and is somewhat less well characterized quantitatively with relevant analytical methodologies and software developed "in-house". Much of what follows related to the MS 2000 constitutes original approaches to extracting information from a multi-beam system.

Initial Data Reduction

EK60

For the EK60 echosounder little data reduction or compression was applied prior to analysis, the exception being rejection of files containing no information on the transects of interest. Data files were first combined into one continuous track for scrutinizing within Echoview. Once combined, the sections of the file that related to specific transects were defined as "regions" and labelled accordingly. Table 2 identifies the individual transects and labels. Two target range boundaries were established for the editing of the EK60 data: The first 1.5 m below the transducer (120 kHz) face and the second 0.5 m above the sounder-detected bottom. All backscatter outside this vertical (i.e., top and bottom) bounded zone was excluded from further analysis. Additional fixed vertical intervals were established for depth specific analyses. Extraneous acoustic targets such as the turbine superstructure and turbine-associated turbulence were identified and excluded from fish backscatter calculations.

MS 2000

The MS 2000 has several output data format options, each imposing inherent limitations on subsequent processing and analyses. For this study we selected the raw elemental data (i.e. non-beamformed) ".smb" output format which offered the greatest analytical flexibility. The MS 2000 multi-beam data files were subsequently converted from non-beamformed to beamformed format in successive 1000 ping groups – using existing in-house software. Data files were also beamformed using an alternative non-linear technique (Cochrane 2002) to determine if the technique improved fish detection. Cursory inspection showed that the non-linear processing yielded "cleaner" – less noisy appearing visual fan sections, but clearly revealed no additional fish echoes. Consequently, it was decided to proceed with the linearly beamformed data because of its superior quantification potential even though these contained periodic noise bursts of unknown origin. Possible sources of this noise prominent in the linear data stream were interference between the two non-synchronized Simrad sounding systems and acoustic Doppler current profilers (ADCP's) mounted on the turbine. These noise bursts were effectively suppressed by specialized algorithms during analysis as described below.

Data Processing

EK60

General: Once the regions (transects) were defined in the data files and the vertical analysis intervals identified, a third variable depth boundary was manually established defining the upper margin of a layer that included all valid observations lying below the surface bubble backscatter zone. This required careful scrutinizing of the echogram to separate areas of surface backscatter noise from areas containing potentially un-obscured fish targets. Fig. 7 illustrates the boundary layers and demonstrates the subjective nature of assigning this boundary. Depth intervals of 5 m were established between the sea surface and the varying depth bottom boundary for subsequent quantification. Backscatter for the entire water column and the vertical intervals were estimated following standard acoustic procedures in the Echoview software. Output options for backscatter included volume backscattering strength (S_v), Nautical Area Scattering Coefficient (NASC), area backscattering coefficient (ABC), and area backscattering strength (S_a). Most estimates of backscatter for the EK60 were expressed in NASC units where the difference between S_a and NASC is simply a scaling factor. A total of 26 transects were extracted from the echogram data and subjected to analysis and variable output.

TS estimates: The Echoview acoustic editing software contains a module that uses standard algorithms to detect individual targets based on a series of input parameters. The output is the target strength distribution of those reflectors which meet the selection criteria. Although the detection of single targets during vessel transit is far more difficult than when stationary due to reduced target redundancy, and generally leads to the selection of fewer echoes, it is still possible. However, it should be noted that the selection of targets is very sensitive to the threshold values used to determine whether an echo originates from a single or multiple target(s) within a sample layer. Information on the distribution of target strength for high probability single-target echoes can be used to infer fish size and possibly species.

The data present in this report represents a “first cut” at the detection of targets and their associated target strengths using general acoustic properties criteria. Refined analysis will be undertaken in the future and values may change slightly. For the initial filter a TS acceptance range of less than -60 dB and greater than -30 dB was used to exclude targets from the analysis unlikely to represent fish. The target echo pulse length amplitude discrimination level was set to 6.0 dB with a minimum normalized pulse length acceptance criteria of 0.6 and a maximum of 1.5. The maximum acceptable split-beam off-axis amplitude compensation was 6.00 dB and the maximum standard deviation of the major and minor-off-axis target angles between multiple ensonifications was specified as 0.6. As a final filtering criterion, only targets with a < 3 dB difference between the compensated and uncompensated TS were included in the summary.

MS 2000 Multi-beam

General: Analysis and the extraction of quantitative data were far more complex for the MS 2000 multi-beam than for the EK60. Quantitative editing and analytical software tools were either not commercially available or sufficiently expensive to force development of in-house tools to analyse and summarize data from the multi-beam system. The analytical process and procedures for the MS 2000 data are presented below.

Time Base: To utilize the data in conjunction with the EK60, logging times were synchronized. MS 2000 data at origin were time-stamped from the time base of the logging computer. This time base displayed both a time offset and a linear offset drift from the EK60 time base. An algorithm was developed to harmonize MS 2000 time to EK60 time to within 2 s over the logging period. This correction was incorporated into subsequent MS 2000 analysis.

Fish Density: Estimates of fish concentrations (fish/m^3) as functions of depth with minimal effects from the presence of backscattering bubble clouds and extraneous noise bursts can be obtained by manually identifying and counting fish echoes in defined depth intervals over a predetermined number of successive fan sections (i.e. pings), then dividing total depth interval fish counts by the total effective ensonified (i.e. observed) water volumes for the relevant depth intervals. This was achieved in a semi-automated manner by manually mouse clicking on visually identified fish echoes on successive fan sections. For each selected echo the port-starboard echo position and depth, and computed echo latitude and longitude were logged for future reference assuming vessel heading to be the same as the direction of travel. The approximation to vessel heading was not particularly good in strong tidal streams, but the only measure available (neither vessel heading nor heading-derived geographic fish coordinates were utilized in the analyses of this report). An associated ancillary file of ping-by-ping maximum available profiling ranges was also generated by mouse clicking on the nearest point on bottom including the leading edge of any turbine echo when present. Because of the laborious nature of target-by-target manual identification it was only practical to apply the technique to a few critical or representative data selections. The detailed theory and implementation of this technique as well as a consideration of its limitations is discussed in APPENDIX I.

Volume Backscattering Strength: Volume backscattering strength (abbr VBS – symbol S_v) is a standard quantitative backscatter measure widely employed in conventional single beam acoustic fish surveys, including, split-beam sounders like the EK60. VBS is a measure of the acoustic intensity returned or "backscattered" from 1 m^3 of ensonified water reduced to a 1 m equivalent observation range using a unit intensity ensonifying source. VBS is a challenging quantity both to measure and to interpret in terms of real-world fish densities and biomass distributions (MacLennan & Simmonds 1992, Clay & Medwin 1977). Computationally, VBS at a given observation range reduces to the suitably scaled, 2-way propagation loss corrected, squared amplitude of the backscattered echosounder signal, divided by the volume of water instantaneously effectively

ensonified – this water volume constituting a fraction of a thin spherical shell at the observation range of thickness equal to one-half the product of the echosounder pulse length and the sound speed. The main difficulty lies in determining the "effective" fraction of the shell that is instantaneously ensonified. This is a function of the spatial properties of the overlapping transmit and receive beam patterns. In modern multi-beam systems some or all of the beam patterns are electronically synthesized and differ for each fan beam.

Two inherent advantages of VBS utilization are: 1) VBS has a precise mathematical/physical definition abetting careful quantification 2) VBS evaluation can be more readily automated for assessment of large datasets than the more subjective manual target identification processing. VBS evaluation also has its operational challenges: First, extracted VBS is a lumped measure of backscatter from all sources including bubble clouds (highly prevalent in the tide-rips of Minas Passage) as well as fish. Exclusion of bubble backscatter by manual editing, as employed with the EK60 split-beam, is impractical considering the multiplicity of 2-D fan sections. Secondly, VBS also contains instrumentation and ambient noise components unrelated to backscatter. Thirdly, derivation of precise fish densities from averaged VBS vs. depth profiles requires knowledge of fish acoustic target strengths at non-dorsal ensonification angles as well as a statistical description of ensonification angles for each depth interval. Note that VBS can serve as a precise, as opposed to an approximate proxy for fish concentration only if all relevant targets have identical target strengths independent of depth and ensonification angle (never the case) or if a suitable "average" target strength can be defined for each depth interval, a complex task for multi-beam systems.

As alluded above, VBS estimates are very sensitive to the presence of noise. Several differing sources of non-fish backscatter origin noise were identified in the MS 2000 field data. To minimize transient noise signal processing algorithms were developed to recognize and cancel brief, periodic, high level noise bursts observed on the linearly beamformed fan sections and these algorithms incorporated into the signal processing. The operative principle was that strong extraneous noise bursts overload the multibeam receiving array preamps. This effect negates normal beamformer operation, resulting in spurious high level beamformer outputs simultaneously affecting all or an appreciable fraction of the synthesized fan beams between specific range limits defined by the temporal character of the noise. Time domain addition or "stacking" of simultaneous fan beam amplitudes followed by application of a carefully chosen trigger threshold allows these noise bursts and their temporal character to be identified, allowing all fan beam outputs to be appropriated blanked in an automated manner.

Amplitude thresholding, i.e. zeroing all beamformed signal amplitudes falling below a predefined level, is a standard acoustic practice to effectively boost signal-to-noise levels when evaluating a desired VBS component arising from fully resolved (i.e. non-overlapping) fish targets. The procedure can usefully minimize the cumulative effect of low level non-fish origin noise, such as noise radiated from the ship or generated internally from the sonar electronics including spurious offsets in system DC zero levels, as well as undesired low level zooplankton backscatter. Thresholding is especially

effective in enhancing the signal-to-noise ratio of fish signals when S_v is to be averaged spatially and/or integrated in the vertical to produce columnar S_a. Thresholding was implemented in the Minas Passage multi-beam analysis.

The authors have previously published fairly rigorous techniques for extracting VBS from the Simrad MS 2000 (then denoted the SM 2000) multi-beam (Melvin et al. 2003, Cochrane et al. 2003). The earlier SM2000 quantification which used the sonar head circular array in both transmit and receive mode is not directly applicable to the Sept. 2010 configuration which utilized a separate external 1.5^0 transmit transducer in Mills Cross configuration with the circular head receive array. Full system calibration with the very narrow beam head would require measurements in a specialized facility that does not exist locally.

We cannot at present compute the precise VBS for the MS 2000 sonar in its current Mills Cross configuration. However, what can be examined is the mathematical component of VBS which consists of the square of the received acoustic amplitude for each beam as a function of range after application of standard 20 log R + absorption time variable gain (TVG) which both reduces the echo signal to an effective observation range of 1 meter and normalizes for the varying area of the instantaneously ensonified water shell with range. The true VBS will consist of this quantity plus multiplicative scaling factors to compensate for the increased beamwidth of the outermost fan beams, the experimentally (test facility) measured departures of the array from idealized beamforming behaviour, and calibration factors derived from the use of a standard acoustic calibration target suitably adjusted for transmit pulse width and non-TVG baseline receiver gain and other variable instrumentation parameters. Nevertheless, simple evaluation of the squared signal amplitude of each beam as a function of range suitable binned by depth, averaged over the entire fan of beams, and in our specific case corrected for a variable sonar pulse width, can serve as a useful indicator of the presence, vertical location, and comparative along-profile density of any fish layers remaining at near constant depth. The comparative intensities of layers at greatly differing depths cannot be reliably extracted with this simplified technique due the missing additional terms. All 16th September multi-beam data were analysed using the simplified VBS approach. Data acquired directly over or very close to the turbine where diffractions and strong exit plume effects might be expected were excluded from analysis - as also with the EK60 processing.

RESULTS AND DISCUSSION

EK60 SPLIT BEAM

Backscatter levels

The initial step in the analysis of the EK60 data was to examine the backscatter throughout the water column including the near-surface backscatter “noise” below 1.5 m believed to originate from bubble clouds. Immediately obvious are the large declines in individual transect backscattering averaging 99.65%, ranging from 98.10% to 99.97%,

when the surface noise zones are removed from the analysis (Table 3). This clearly illustrates the significance of the backscatter that is attributed to surface bubble entrainment – the degree of which varies dramatically throughout the tidal cycle. Peak near-surface backscatter amplitudes and the deepest vertical penetrations of the surface backscatter generally correspond with maximum tidal flows around the turbine, however, there are spatial differences reflected in the inter-transect variability. Although the surface noise was relatively strong there was no evidence of acoustic shading of the water column or of the bottom below the noise.

Based on the water column NASC (Nautical Area Scattering Coefficient) the strongest total backscatter for a single pass occurred in Transect 4 which encompassed the turbine (Table 3). This was followed by Transect 6 and Transect 7 with transects (T3 and T5) closest to the turbine having a maximum backscatter of about 66% the T4 maximum. Generally speaking the backscatter was weaker in transects to the north and south of the turbine with the latter slightly stronger than the former. The largest component of backscatter appears to originate from tidal/wind generated surface bubble clouds. Examination of the backscatter after exclusion of visible bubble clouds produced a similar pattern with the strongest NASC originating along the transect which passed over the turbine, except for Transect 5 located just south of the turbine. Transect 5a, which produced the highest overall backscatter, corresponds to the period of strong ebb flow and the observation of a layer of targets at about 15 m. This is consistent with the multi-beam observations below.

Examination of the backscatter by depth and transect illustrates a system that is extremely variable from one location to another, but one that does have some structure that appears to be linked to the tidal cycle (Figs. 8, 9, and 10). It should be noted that while there are measurable quantities of fish-like targets throughout the water column the number of fish/100 m^2 could be considered sparse. Estimates of fish number from the Area Backscattering Strength (S_a), assuming a 15 cm clupeid (TS = -48.38), averaged 2.2 fish/100 m^2 to bottom over all transects and ranged from 0.5 to 6.5 fish/100m^2 depending upon the specific transect.

Only two runs over each transects (T1 to T3) north of the turbine were undertaken during the one day survey. All three transects show intra-tidal variability with respect to the distribution of backscatter as represented by the proportion of backscatter in Fig. 8 and the level of backscatter by depth. In essence, Transect 1 characterizes the observed bimodal distribution of fish-like targets at 10 - 15 m and 35 - 40 m and how the backscatter levels change with the tide. Each individual transect clearly shows a peak in fish-like targets at approximately these water depths. The depth and strength of the mode changes for a specific transect depending upon the tidal cycle. One mode occurs at a depth just above the current turbine top and the other mode at depths that would potentially interact with the turbine. Backscatter amplitudes can vary by a factor of 4 to 5 within a specific transect between runs (i.e., time), and 2 to 3 times between different transects sampled closely in time (Fig. 8). More structure might be discerned if depth intervals smaller than 5 m were used.

Similar patterns in the distribution of backscatter were observed for the transects occupied south of the turbine where three runs were conducted for each line (Fig. 9). Again, two primary modes in target depth distribution occurred at about 10 - 20 m and 25 - 30 m depending upon the survey time. However, there was a marked difference in the backscatter amplitudes for Transect 5, and possibly Transect 6, compared to Transect 7 and those north of the turbine. For Transect 6 it is likely, given the high amplitude occurring in the 0 - 5 m depth interval that one or more strong targets, likely bubble clouds, did not get removed from the analysis. However, on closer re-examination nothing could be discerned. The highest backscatter in Transect 7 occurred just at the turn of the tide. Note backscatter amplitudes (with surface noise removed) at, or shortly after slack water, are in the order of 10 - 20 times less than those observed during the ebb tide. Occasionally a third peak appeared at water depths of about 40 m in some of the transects, a depth which lies below the depth of the current turbine.

Transect 4 was occupied (10 runs) more than any of the others and provides observations for most of the ebb, and the early stages of the flood, tide. The data are split to balance NASC levels into two periods; the ebb tide to slack (Transect 4a-f) and the slack to flood (Transect 4g-j) for presentation (Fig. 10). As with the other transects two primary modes were observed in the water column which varied depending upon the tidal cycle. The maximum backscatter occurred in the 10 - 20 m depth interval and was observed about 1 hour into the ebb. Thereafter, the backscatter gradually diminished to slack water. A similar pattern was observed throughout the rest of the water column with a secondary peak in backscatter occurring at 30 - 35 m depth. A third peak sometimes occurred at approximately 40 m in the deeper sections of the transect.

After slack water the amplitude and the distribution of backscatter changed dramatically. First the amplitude of the NASC was reduced to <10% of the values observed before slack water. Modes in distribution occurred at similar depths but the highest backscatter occurred in deeper water as the flood tide began. There is a slight suggestion the fish-like targets may have moved up in the water column as the tidal flow increased (Fig. 10).

Target Strengths

The target strength values from the survey were pooled and summarized into 4 broad area/time intervals; those north of the turbine (Transects 1-3), those south of the turbine (Transects 5-7), those on the turbine line during the ebb tide (Transects 4a-f) and those during flood tide (Transects 4g-j). Overall 1,033 individual targets were identified during the survey. The target strength distribution was broad ranging from -60 dB to -35 dB although there were only 2 targets detected between -37 dB and -30 dB. The data were however skewed to the left and dominated by weaker targets (Fig. 11). Several modes are also apparent in the distribution. By far the largest mode occurred between -59 dB and -56 dB, followed by between -55 and -52 dB, and then -51 to -47 dB. The remaining targets are spread over -45 dB to -38 dB.

Originally it was thought the peak occurrence of targets in the -55 to -60 dB range was related to air entrapment in the turbulent near surface waters. Plotting of the TS values

by depth indicates that there was no real segregation of TS related to water depth. TS values associated with a peak are found throughout the water column. Close examination of the data also reveals the distribution TS corresponds with the occurrence of the water depth backscatter modes (Fig. 12).

Detailed examination of the TS distribution by transects and area shows variability over time (Fig. 13). Transects with the largest number of detected targets show the broadest distribution (T4a-f) and the patterns appear to be similar for transects north and south of the turbine for TS < -44 dB. Larger targets appear to occur in the deeper waters south of the turbine. Comparison of the TS during ebb tide and during the flood (incomplete coverage) illustrates a real lack of larger TS's >-55 dB. However, this may not have been the case if sampling had continued further into the flood tide.

In general, acoustic targets greater than -60 dB are considered fish with TS being dependent upon the length and species of fish. Unfortunately, the information collected to date does not permit any reliable identification of species, yet species within observed TS dB ranges are known to occur in the area at the time of sampling. Any reference to species is purely speculative. Given the observed TS distributions it is likely that the targets with a TS < -52 dB represent relatively small fish in the order of 10 cm or less (e.g. young of the year gaspereau or herring). The two modes in this range may represent two or more species or size groups. TS distributions in the range of -51 to -47 dB are characteristic of juvenile clupeids in the 15 - 20 cm range (e.g. juvenile herring- age 1+). A TS in the range of -46 to -41 dB represents larger and likely adult fish such as herring, gaspereau, or smelt. The few targets with a TS > -40 dB are most probably one of several groundfish species known to occur in the area or a migratory shad/striped bass.

MS 2000 MULTI-BEAM

General

Visual inspection of 16th Sept. multi-beam fan sections (Fig. 14) and aerial multi-ping sections (Fig. 15) revealed distinct and abundant fish targets in the upper 10 - 20 m of the water column over a significant fraction of the survey, with occasional targets observed deeper all the way to bottom (depths are reported relative to the transducer depth of about 2 m). Fish within the 10 – 20 m depth interval frequently displayed noticeable short range aggregation tendencies as seen, for example, in Fig. 14 right of center.

As was the case for the EK60, bubble clouds were observed extending from the surface occasionally to depths of 20 m or more; an observation consistent with those from the earlier pilot survey (Melvin et al. 2009). Differences in backscatter character between bubble clouds and fish aggregations were sometimes subtle, making them difficult to distinguish visually on echograms. This would also tend to render any fully automated identification of fish targets problematic.

Fish Density

At the time of the current report multi-beam manual target selection analysis has been limited to two exploratory turbine-transiting profiles due primarily to the laborious nature of this process. The first profile consisted of 1700 fan sections extending from 12:33:11 to 13:01:11 GMT covering most of line T4a while surveying west-to-east against a strong ebb flow. Fish echoes appeared particularly numerous around the 15 m depth mode. Coordinates of about 31,400 individual fish echoes were logged for an average of 18.5 fish per section. The second profile consisted of 529 fan sections recorded from 16:08:53 to 16:17:37 GMT and covering most of profile T4f while surveying west-to-east just prior to the end of the ebb cycle (slack low tide interval). The second profile was characterized by markedly lower visual fish densities in the ~15 m depth range. Only 1450 fish targets were observed over the second section for an average of about 2.7 fish echoes per section. Note that the maximum effective profiling range is limited to the water depth below transducer so smaller water volumes per fan section were sampled on the second profile due to the reduced tidal height; nevertheless, the lower fish densities were still predominant.

Fish densities (fish/m^3) as functions of depth, were computed for a series of 2 m vertical bins extending from the transducer depth (2 m) to a maximum profiling range defined by the minimum transducer to bottom distance over successive groups of usually 100 pings. To accomplish this, for each individual ping the effective sonar-sampled water volume was calculated for each discrete 2 meter vertical depth interval out to a defined maximum effective profiling range by means of hybrid analytical-numerical integration (Appendix I). The relevant ensonified water volumes for each depth interval were then summed over the 100 ping sub-interval. The total number of fish counted for each 2 m depth interval over the same 100 ping interval was then divided by the corresponding accumulated sonar-sampled water volume to yield fish density. Note that this methodology remains valid regardless of the degree of successive ping volumetric overlap or even in the total absence of any such overlap - the degree of overlap normally varies with observation range. Nor does the technique require tracking of specific targets between successive pings to eliminate counting redundancies – an uncertain task without beam stabilization. As discussed in Appendix I, the uncertainty and limitations of this approach, mainly arise in assigning the effective fore-aft (out-of-fan) beam width to defining the effective observed water volume. Choice of an appropriate fore-aft beam width depends on how far into the ambient noise background a fish echo can be reliably discerned. For manual extraction this depends on fish target strength, target clutter (noise), and operator subjective factors. Because of these multiple considerations an inherent uncertainty factor of about 2 in absolute multi-beam derived fish densities is likely, but the technique does have the advantage of excellent rejection of bubble cloud backscatter. Selected examples of fish density analysis are shown in Figs. 16(A) and 17(A) for 100 ping sequences recorded on two differing portions the ebb tide cycle, the first for a period when fish targets in the 15 m depth range appeared especially numerous. It should be noted that the fish density profiles plotted have been scaled to an “effective” out-of-fan target detection beamwidth of 1^0. The true effective beamwidth, as discussed in Appendix I, is difficult to assign but may be of the order of 3.75^0. In this case the

actual fish densities will be reduced from those plotted by a factor of $\sin(3.75^0/2)/\sin(1^0/2) \sim 3.75$

Volume Backscattering Strength

Volume backscattering strength (S_v) is defined as the ratio (in either linear or decibel form), of the intensity of the backscattered sound from a unit ensonified volume at a reference distance of 1 m to the intensity of the incident sound source. In its linear form, S_v is directly proportional to target density for the ideal instance of all fish targets backscattering identically (i.e. possessing identical target strengths). An example of simplified (no beam pattern corrections) S_v extraction applied to the identical 100 ping data series of Fig. 16(A) is shown in Fig. 16(B). The similarities between fish density and S_v profiles between 10 and 20 m depths are to be noted. The inherent difference between these two measures is that the S_v profile includes backscatter contributions from surface bubble clouds and other non-fish sources, real or spurious, which for the case of the fish density profile of Fig. 16(A) have been largely eliminated by the manual target selection process. Fortunately, in the example shown the bubble cloud backscatter peaks at sufficiently shallow depths that deeper fish origin S_v levels, are only modestly affected. A comparison data series collected near the end of the ebb tide cycle, when fish densities around 15 m depth appeared much lower is shown in Fig. 17(B). It should be noted that a high degree of noise reduction must be applied to these data and the current results are very sensitive to the algorithms chosen and the "fine tuning" of their parameters. The fairly good discernment of fish layers by S_v analysis shown in Fig. 16 should not be considered representative of the bulk of data collected when fish densities were lower.

Much potential exists for improvement of the noise removal algorithms. Nevertheless, we believe that that even the simplified S_v analysis at its current state of development when applied judiciously to the Minas Passage data furnishes useful information about presence, density, and vertical structure of at least the shallow fish mode, a conclusion supported by analysis of the remainder of the collected sections. Resultant S_v peak linear amplitudes for the ~15 m centered modal fish layer scaled from successive plots analogous to Figs. 16(B) & 17(B) are shown in Fig. 18 for the full duration of the survey (only peak fish layer S_v amplitudes can be reliably separated from the bubble cloud scatter in the majority of cases). A unit amplitude sinusoidal approximation to the Cape Sharp tidal amplitude is also included in Fig. 18.

While a peak in S_v in the depth range centered on 15 m depth is a reasonably persistent feature in the survey, concentrations displayed in Fig. 18 are observed to peak sharply between about 12:35 and 13:15 GMT – a roughly 40 min time interval centered about 2 hr 34 min into the ebb tide cycle. Fish are present earlier but in markedly lower concentrations, and present later in lower and generally declining concentrations extending over the remainder of the ebb tide cycle. On comparing survey tracks with the time-varying fish concentrations in Fig. 18 it is not immediately evident that concentrations are strongly correlated with location relative to the turbine. While concentrations appeared to be consistently lower on transects north (shoreward) of the turbine this may have been more a function of when these transects were steamed rather

than their location. Fish were present below the 15 m modal layer but in much lower concentrations than the peak values observed near 15 m depth. For depths below 15 m, the limited set of concentrations derived from direct counting probably constitute the more reliable data on vertical fish density distribution since the much longer duration S_v data coverage may be contaminated by residual bubble cloud noise below 15 – 20 m. The current lack of beam pattern corrections in the "simplified" S_v analysis also makes comparison of fish densities between widely varying depths suspect. Fish species, hence target strengths, may also vary between shallow and deeper fish concentrations.

Species interpretation of the fish concentrations of Fig. 18 must remain speculative; target strengths are not readily extractable from multi-beam in contrast to split-beam systems. Also, the MS 2000, unlike the EK60, is presently un-calibrated in an absolute sense. Some clues are furnished by the EK60 target strength statistics reported above. Limited ground truth also exists in the form of 9 trawl samples taken in the Minas Passage area on the 16 & 17th Sept. 2010 by CEF Consultants (CEF Consultants 2011) during a parallel combined trawl/acoustics survey. Eight (8) of 9 trawl samples were dominated by herring. The trawl having the highest herring concentration was set west of the turbine site in relatively shallow water (60 m) with a headline depth between 9.1 and 18.3 m and sampling centered 2 hr 33 min into the ebb tide cycle (essentially the same tidal phase where acoustic concentrations were noted to peak above). However, the trawl sampling was on the night time ebb tide while our acoustic observations were conducted on the preceding day ebb cycle.

Since the geographic locations where the highest multibeam fish concentrations were observed (Fig. 18) are reasonable proximate, and since the average shallow current during the period was roughly of the order of 2.5 m/s, the along-channel spatial extent of the 40 min. duration enhanced fish concentration, if moving totally passively, would be of the order of 2400s x 2.5 m/s = 6000 m. The highest fish concentrations were observed to have largely passed the survey area prior to maximum ebb flow which, disregarding local current perturbations, would be expected near 13:30 GMT. It could be that a loose juvenile herring assemblage is using the ebb current cycle to systematically move from the Minas Basin into the open Bay of Fundy. On the other hand one could be observing a more random or repetitive phenomena where the fish advect back through the survey area - or another portion of the Passage cross section - on the following flood tide cycle. Clearly, this question requires further investigation. Of further interest is the observation that at 13:26 GMT, near the end of the period of highest fish density, the acoustic depth, from the transducer to the top of the turbine, was 19 m. Because the tide was continuously declining during the period of high fish density, the vast majority of the fish observed during this critical period should have passed over the top of the turbine thereby minimizing any interaction.

TURBINE OBSERVATIONS

The OpenHydro turbine was clearly imaged on both acoustic systems; the MS 2000 multi-beam (Fig. 19) clearly revealed its circular shape as well as its supporting base. Occasional fish echoes could be observed to within about 5 m of the turbine on both

systems. On the MS 2000 fan sections, observation of turbine-proximate fish echoes was largely restricted to waters immediately above the turbine since strong diffraction fringes extending out from the turbine shroud effectively obscured the water volumes immediately adjacent to the turbine nacelle openings. On the EK60 echograms prominent acoustic wakes were observed on the downstream side of the turbine with a hint, perhaps, of some flow disturbance close to the turbine on the intake side. This very proximate intake-side effect is difficult to reliably separate from superstructure diffraction (Fig. 20). Near slack tide, downstream wakes angled up steeply toward the surface suggesting a buoyant nature, conceivably originating from turbine or turbine enclosure induced aeration or cavitation. On the multi-beam sections, wakes on the outlet side of the turbine were also frequently visible – perhaps less dramatic in appearance then those recorded by the EK60 (see above) due to the multi-beam's lower sensitivity – but curiously, in some cases, suggesting the form of hollow circular arcs in 3-D space. Hollow arcs generated from turbulent interactions with the outer enclosing shroud alone, might be consistent with all turbine blades being absent at the time of observation – a hypothesis consistent with what is otherwise known about the structural failure of the turbine blades.

CONCLUSIONS

The following conclusions were extracted from the 2010 single and multi-beam acoustic observations in Minas Passage. The above-reported observations are based on a single survey which elucidated primarily the ebb tide with observations confined to daylight hours. Temporal and spatial variability will likely be observed as more surveys are completed. Additional surveys are scheduled for 2011/2012 and should provide a more representative sampling of seasonal and diel variability.

1) Conventional surface acoustic technology can be used to detect fish distribution and abundance throughout the water column below the bubble-dominated surface noise zone. There are, however, some concerns in the detection individual fish in or near the surface waters.

2) Combining single beam with multi-beam observations which ensonify much higher water volumes enhances the ability to detect and define layers of fish, especially near-surface. In several cases, layers of fish were detected by the MS 2000 that were not, or may not have been, identified as fish during the EK60 editing. Considerable work is still required to optimize the MS 2000 noise suppression algorithms for more reliable extraction of volume backscattering. Single targets near the surface noise zone were difficult to discern.

3) Acoustic targets were generally observed at 2 backscatter-defined modal depths; between 10-20 m and 30-40 m. The precise modal depth varied depending upon the tidal phase. Occasionally a third mode was observed in the deeper water portions of transects.

4) There appeared to be differences between the EK60 and the MS 2000 datasets in regard to which modal depth interval was of greater amplitude. Relatively speaking, the EK suggested that the deeper mode was greater than the shallower and this is probably the most reliable conclusion: The MS was not optimized to detect volume backscattering from deeper targets nor fully normalized to compare backscattering between widely separated depth intervals. Regardless, both systems showed peaks in backscatter at the same depth intervals.

5) There appeared to be a distinct period during the ebb tide when fish preferentially transited out of the basin. This perception may, however, change with additional surveying.

6) Overall, the density of fish was relatively low at the time of surveying based on the observed volume backscatter (**S_v**) levels from the EK60.

7) If these technologies are to be used as monitoring tools automated methods must be developed to enhance what is now labour intensive scrutinizing.

RECOMMENDATIONS

While intriguing patterns of fish behaviour have been revealed in a single acoustic backscatter survey of less than 1 tidal cycle duration, much more extensive surveying in the temporal domain is required to draw definitive conclusions about potential impacts of TISEC devices on the behaviour and mortality of upper Bay of Fundy fish stocks.

Approximately 7 vessel acoustic surveys of a full tidal cycle in the now vacated TISEC test area are scheduled for 2011 and 2012. The small number and brevity of Minas Passage sampling cruises presently planned will require skilful survey time selection based on the existing, but fragmentary scientific data, coupled with a measure of informed speculation in order to ensure an adequate and representative description of the fish ecosystem composition, its functioning, and, especially, its vulnerabilities. The authors are currently contemplating deployment of an autonomous, stationary, bottom-mounted echosounder to extend monitoring into the inter-survey periods. Such continuous, longer-term acoustic monitoring would have several innate advantages even in the absence of the detailed spatial and target strength data possible from ship-based surveys:

1) The ability to ascertain if “spot” vessel-based acoustic surveys are representative of longer term ecosystem conditions, especially in regard to fish densities, and fish vertical distributions, and repetitive behaviours.
2) The ability to separate tidal current induced fish behaviours from those induced by diurnal variations in ambient light levels i.e. linked to time of day.
3) The detection of significant “transient” biological events – if they exist.

Better quantification of the existing multi-beam sonar and its beam patterns is both possible and recommended to generate more accurate vertical profiles of S_v and to enable more precise inter-comparison with complementary data from split-beam systems.

Trawl survey ground-truth is definitely required to support acoustic-based interpretation. Fish target strength data can be useful but without supporting ground-truthing it often remains too ambiguous for confident species identification. Trawl surveys recently conducted in the general Minas Channel area seldom sampled below about 20 m depth resulting in our current knowledge of fish distributions being highly biased toward the near-surface region. This should be rectified.

While observation of fish densities in the general vicinity of turbines can at best place upper limits on turbine fish transits, acoustic methodologies employing surface vessels are unlikely to detect active turbine avoidance by fish occurring within several meters of the intakes. This critical proximate to the turbine constitutes a challenging observational region for conventional shipboard systems where individual fish echoes are normally obscured by strong acoustic beam side-lobe scattering and multibeam array sensor overloads from the turbine structure and where stable positioning and sufficiently long observation times are also difficult to achieve – not to mention the compounding problem of additional fish avoidance from noisy vessels. If fish are repelled at ranges of 10's to hundreds of meters by noise radiated from tidal turbines some potential for vessel-based detection may exist. However accurate and dependable delineation of avoidance would seemingly require acoustic systems to be mounted directly on the turbine structure, looking outward at optimum observation angles, with hard-wired power and telemetry to shore. The practicalities of mounting (and recovering) general purpose scientific instrumentation on turbine structures should be addressed. It should be noted that even if turbine fish transits can be eventually quantified, ecosystem impacts can only be accurately evaluated if additional transit mortality data are available. However, even in the absence of the latter parameter, quantification of fish avoidance should enable a reduced upper bound to be placed on potential fish mortality compared to that derived from utilization of fish densities and turbine flow rates alone.

ACKNOWLEGDEMENTS

The authors would like to acknowledge the crew of the Huntsman Marine Science Centre research vessel the *Fundy Spray* for their cooperation and help during this first survey in a very trying environment. Art MacIntyre, Nicole Gear, and Sarah Scouten provided technical support for the equipment setup and mounting. Nova Scotia Power funded the vessel charter. This project was co-sponsored by the Science Branch of Fisheries & Oceans, Canada and the Offshore Energy Environmental Research Association (OEER).

REFERENCES

AECOM. 2009. Minas Basin Pulp and Power Volume 1: Environmental Assessment Fundy Tidal Energy Demonstration Facility. AECOM Canada Ltd. 1701 Hollis Street, SH400 (PO Box 576 CRO), Halifax, NS, Canada B3J 3M8. 229p.

CEF Consultants Ltd. 2011. Fish Surveys in Minas Channel. Final Report on 2010 Surveys. In: FORCE (Fundy Ocean Research Center for Energy). Fundy Tidal Energy Demonstration Project, Environmental Effects Monitoring Report. September 2009 to January 2011. Appendix H: 53 pp.

Clay, C. S. and Medwin, H. 1977. Acoustical Oceanography: Principles and Applications. John Wiley & Sons, New York. 544 pp.

Cochrane, N. A. 2002. Non-linear Processing to Remove Multi-beam Sonar Artifacts. Can. Tech. Rep. Fish. Aquat. Sci. 2402: iv + 29 p.

Cochrane, N. A., Li, Y., and Melvin, G. D. 2003. Quantification of a multibeam sonar for fisheries assessment applications. J. Acoust. Soc. Am. 114(2): 745 – 758.

Durand, N., Cornett, A., and Bourban, S. 2008. 3D Modelling and Assessment of Tidal Current Energy Resources in the Bay of Fundy. NRC Canada Technical Report CHC-TR-052 April 2008. 110p.

MacLennan, D. N. and Simmonds, E. J. 1992. Fisheries Acoustics. Chapman and Hall, London. 324 pp.

Melvin, Gary D., Cochrane, Norman A., and Fitzgerald, Pat. 2009. Evaluation of Single and Multi-beam Sonar Technology for Water Column Target Detection in an Acoustically Noisy Environment. Can. Tech. Rep. Fish. Aquat. Sci. 2840: vi + 27 p.

Melvin, Gary D., Cochrane, Norman A., and Li, Yanchao. 2003. Extraction and comparison of acoustic backscatter from a calibrated multi- and single-beam sonar. ICES Journal Marine Science, 60: 669-677.

Table 1. EK60 sounder calibration settings used for the 16 Sept. 2010 Minas Passage acoustic survey.

Calibration Settings	Applied	Datafile
Absorption Coefficient (dB/m)	0.04095	0.03744
Sound Speed (m/s)	1493.89	1493.89
Transmit Power (W)	500	500
Two-way beam angle (dB re 1 Steradian)	-20.8	-20.8
Transducer gain (dB)	26.31	25.7
Sa Correction (dB)	-0.34	0
Transmit pulse length (ms)	1.024	1.024
Frequency (kHz)	120	120
Minor-axis 3dB beam angle	6.45	7.1
Major-axis 3dB beam angle	6.45	7.1

Table 2. Summary of acoustic transects conducted in Minas Passage on 16 Sept. 2010. Transects are numbered from north to south. Transect 4 passes directly over the turbine.

Transect	Date	Sounder Frequency	Start Time (GMT)	End Time (GMT)	Tide Phase	Start Time (Local)	Start Lat	Start Lon	End Lat	End Lon	Transect Length (m)
T1a	20100916	120	15:07:52.50	15:13:55.83	E	12:07:52	45.3672	-64.4225	45.3694	-64.43441	958
T1b	20100916	120	18:01:04.45	18:04:57.16	F	15:01:04	45.3693	-64.43419	45.3670	-64.42213	965
T2a	20100916	120	14:53:56.28	15:07:05.95	E	11:53:56	45.3686	-64.4352	45.3663	-64.42245	1045
T2b	20100916	120	17:30:41.89	18:00:19.41	F	14:30:41	45.3662	-64.42165	45.3687	-64.43519	1132
T3a	20100916	120	14:47:16.97	14:52:38.22	E	11:47:16	45.3654	-64.42279	45.3681	-64.43546	1039
T3b	20100916	120	17:24:23.58	17:29:52.35	S	14:24:23	45.3679	-64.43591	45.3656	-64.42229	1083
T4a	20100916	120	12:26:54.61	13:02:02.45	E	09:26:54	45.3669	-64.43287	45.3635	-64.42056	1113
T4b	20100916	120	13:02:12.95	13:07:38.72	E	10:02:12	45.3637	-64.4206	45.3666	-64.43417	1123
T4c	20100916	120	13:08:56.78	13:33:28.08	E	10:08:56	45.3664	-64.43378	45.3645	-64.42338	901
T4d	20100916	120	14:19:19.98	14:45:51.39	E	11:19:19	45.3658	-64.43742	45.3646	-64.4235	1213
T4e	20100916	120	15:16:19.95	15:32:56.83	E	12:16:19	45.3673	-64.43637	45.3646	-64.42327	1097
T4f	20100916	120	16:04:38.95	16:17:14.08	S	13:04:38	45.3653	-64.43875	45.3643	-64.42293	1396
T4g	20100916	120	16:49:35.28	16:59:13.28	S	13:49:35	45.3654	-64.43833	45.3639	-64.42225	1395
T4h	20100916	120	16:59:52.31	17:23:22.02	S	13:59:52	45.3640	-64.4226	45.3671	-64.43582	1124
T4i	20100916	120	18:09:15.39	18:29:01.44	F	15:09:15	45.3645	-64.41874	45.3652	-64.42757	784
T4j	20100916	120	18:29:16.45	18:31:39.08	F	15:29:16	45.3652	-64.42767	45.3644	-64.42365	351
T5a	20100916	120	13:34:20.63	13:38:44.86	E	10:34:20	45.3639	-64.42401	45.3660	-64.4357	945
T5b	20100916	120	15:36:02.97	15:41:39.27	E	12:36:02	45.3640	-64.42381	45.3662	-64.4358	960
T5c	20100916	120	16:18:20.16	16:26:17.58	S	13:18:20	45.3638	-64.42398	45.3661	-64.43571	948
T6a	20100916	120	13:40:04.41	14:11:43.58	E	10:40:04	45.3653	-64.4363	45.3627	-64.42435	1059
T6b	20100916	120	15:43:37.88	15:56:52.03	S	12:43:37	45.3653	-64.43633	45.3625	-64.42434	983
T6c	20100916	120	16:27:35.66	16:35:58.58	S	13:27:35	45.3651	-64.43634	45.3625	-64.42434	972
T7a	20100916	120	14:13:24.17	14:17:31.89	E	11:13:24	45.3618	-64.42533	45.3645	-64.43749	970
T7b	20100916	120	15:58:26.63	16:03:52.41	S	12:58:26	45.3613	-64.4253	45.3647	-64.43759	1020
T7c	20100916	120	16:37:22.66	16:48:38.25	S	13:37:22	45.3619	-64.42534	45.3649	-64.43753	1015

Table 3. Summary of Volume backscattering strength (S_v), Nautical Area Scattering Coefficient (NASC), Area backscattering coefficient (ABC), and Area backscatter Strength (S_a) for each transect with and without the surface noise.

Transect	Noise Included				Noise Excluded				
	Mean Sv	NASC	Area Backscatter Coefficient	Area Backscatter Strength	Mean Sv	NASC	Area Backscatter Coefficient	Area Backscatter Strength	Percent Excluding
T1a	-54.60	6454.6	0.000026	-45.88	-82.21	7.234	0.0000002	-67.75	0.650
T1b	-54.22	6892.8	0.000146	-38.35	-86.71	3.357	0.0000001	-71.09	0.053
T2a	-54.29	7056.0	0.000191	-37.19	-79.24	11.864	0.0000003	-65.60	0.144
T2b	-54.95	5801.3	0.000150	-38.25	-85.16	4.814	0.0000001	-69.52	0.075
T3a	-54.61	6311.8	0.000042	-43.79	-82.30	8.190	0.0000002	-67.21	0.455
T3b	-54.84	5752.5	0.000164	-37.86	-86.48	3.419	0.0000001	-71.01	0.048
T4a	-52.24	9417.5	0.000148	-38.29	-73.66	40.432	0.0000009	-60.28	0.632
T4b	-52.59	8845.2	0.000135	-38.71	-75.38	31.324	0.0000007	-61.39	0.540
T4c	-52.81	8353.7	0.000148	-38.29	-75.25	27.481	0.0000006	-61.95	0.430
T4d	-57.10	2942.4	0.000114	-39.44	-76.16	24.921	0.0000006	-62.38	0.508
T4e	-58.28	2238.5	0.000163	-37.89	-79.56	12.648	0.0000003	-65.32	0.180
T4f	-61.42	1112.5	0.000194	-37.13	-83.28	6.009	0.0000001	-68.56	0.072
T4g	-51.97	9362.4	0.000160	-37.96	-81.89	7.672	0.0000002	-67.50	0.111
T4h	-53.42	6384.0	0.000025	-45.98	-83.75	5.431	0.0000001	-69.00	0.500
T4i	-51.79	6395.1	0.000014	-48.42	-82.63	4.847	0.0000001	-69.49	0.782
T4j	-50.73	9488.7	0.000220	-36.57	-83.09	3.249	0.0000001	-71.23	0.034
T5a	-56.59	3487.8	0.000068	-41.66	-73.01	55.982	0.0000013	-58.86	1.903
T5b	-59.04	1801.2	0.000081	-40.92	-82.72	6.315	0.0000001	-68.34	0.181
T5c	-53.53	6301.7	0.000052	-42.85	-84.48	4.202	0.0000001	-70.11	0.188
T6a	-53.46	7008.6	0.000204	-36.89	-76.56	21.939	0.0000005	-62.93	0.249
T6b	-61.29	1086.7	0.000205	-36.88	-76.87	24.807	0.0000006	-62.40	0.280
T6c	-52.05	8814.1	0.000133	-38.75	-85.05	3.744	0.0000001	-70.61	0.065
T7a	-55.04	4904.9	0.000146	-38.34	-79.02	13.697	0.0000003	-64.98	0.217
T7b	-63.80	619.9	0.000218	-36.61	-85.93	3.347	0.0000001	-71.10	0.036
T7c	-52.51	8231.0	0.000217	-36.63	-85.27	3.673	0.0000001	-70.69	0.039

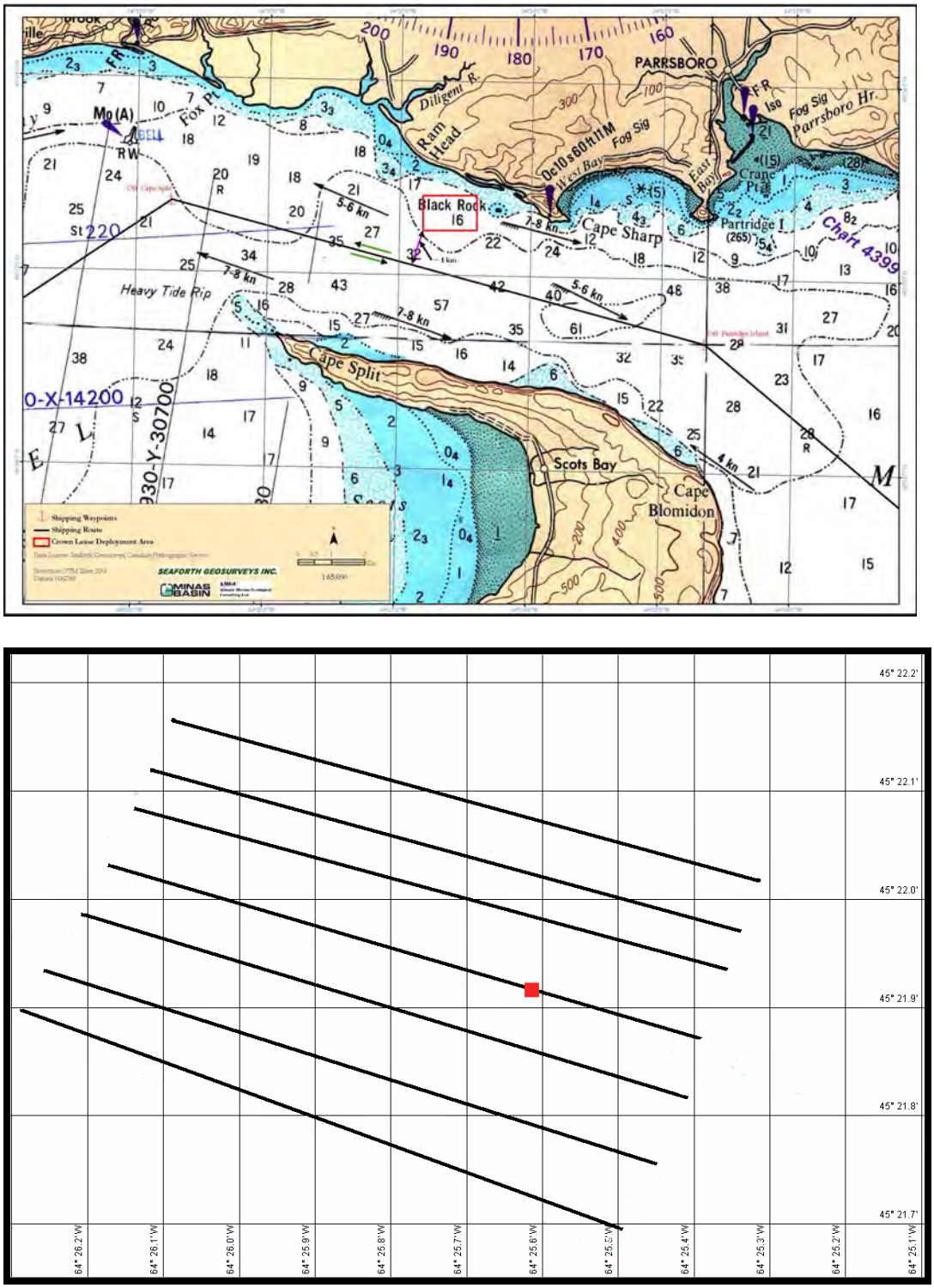

Figure 1. Location of the acoustic survey area/test site in Minas Passage, Upper Bay of Fundy (top) and the general pattern of survey transects (bottom). The position of the OpenHydro turbine is marked with a red dot.

Figure 2. The Huntsman Marine Science Centre R/V *Fundy Spray* approaching the wharf in Parrsboro Nova Scotia.

Figure 3. DFO Research Scientist G. Melvin with boom-mounted acoustic transducer package. The orange unit at top is the 120 kHz Simrad EK60 split-beam transducer. Immediately below it lies the 200 kHz Kongsberg-Mesotech MS 2000 narrow beam, linear transmit transducer. Near bottom is the circular arc MS 2000 receive transducer.

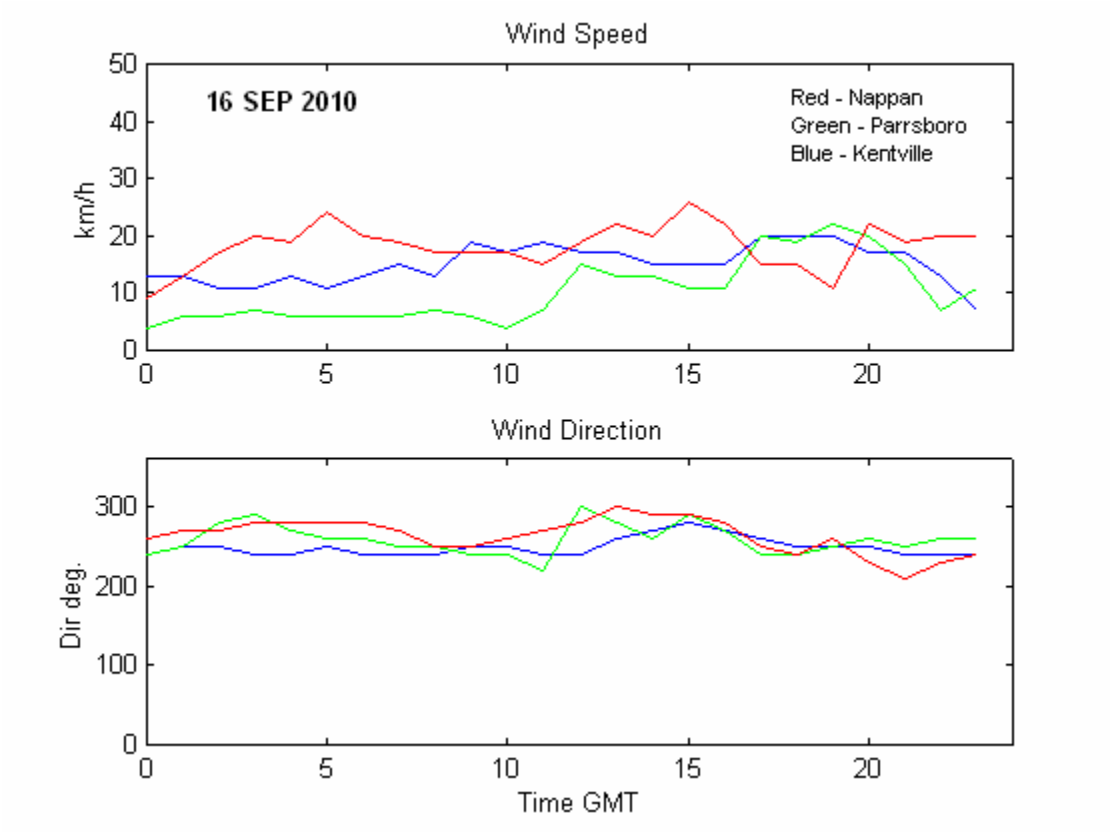

Figure 4. Wind speed and direction for three locations in the vicinity of Minas Passage on 16 Sept. 2010. Source: Environment Canada, National Climate Data and Information Archive.

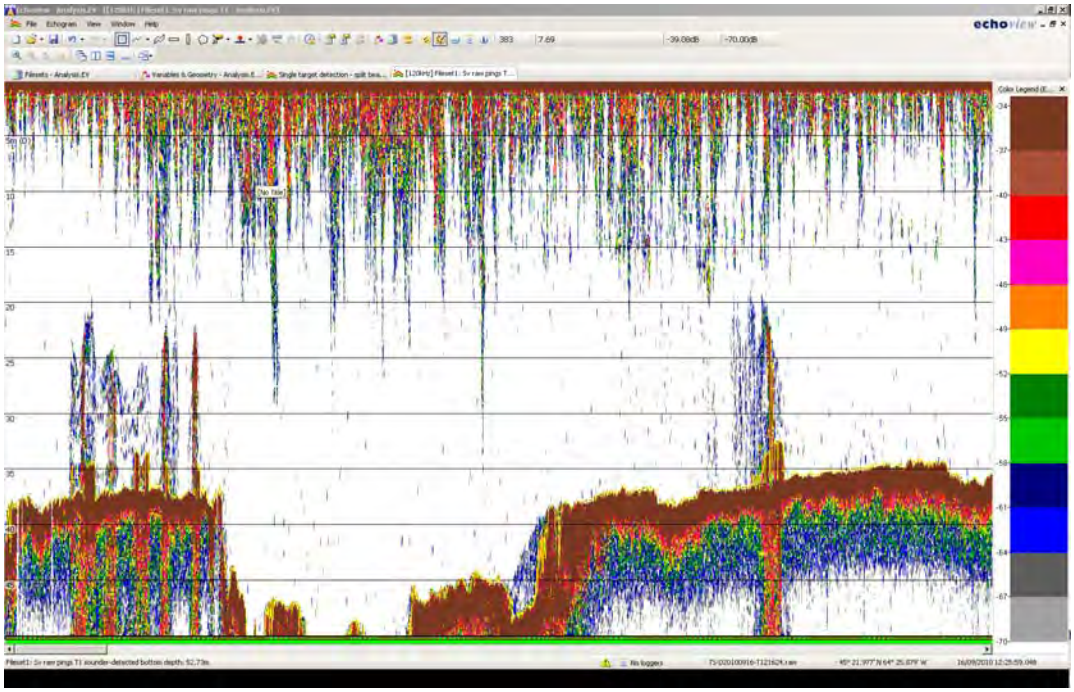

Figure 5. Echogram from the EK60 echosounder showing several passes over the turbine (LHS) prior to commencing the survey and a single pass over the turbine during the first transect (RHS).

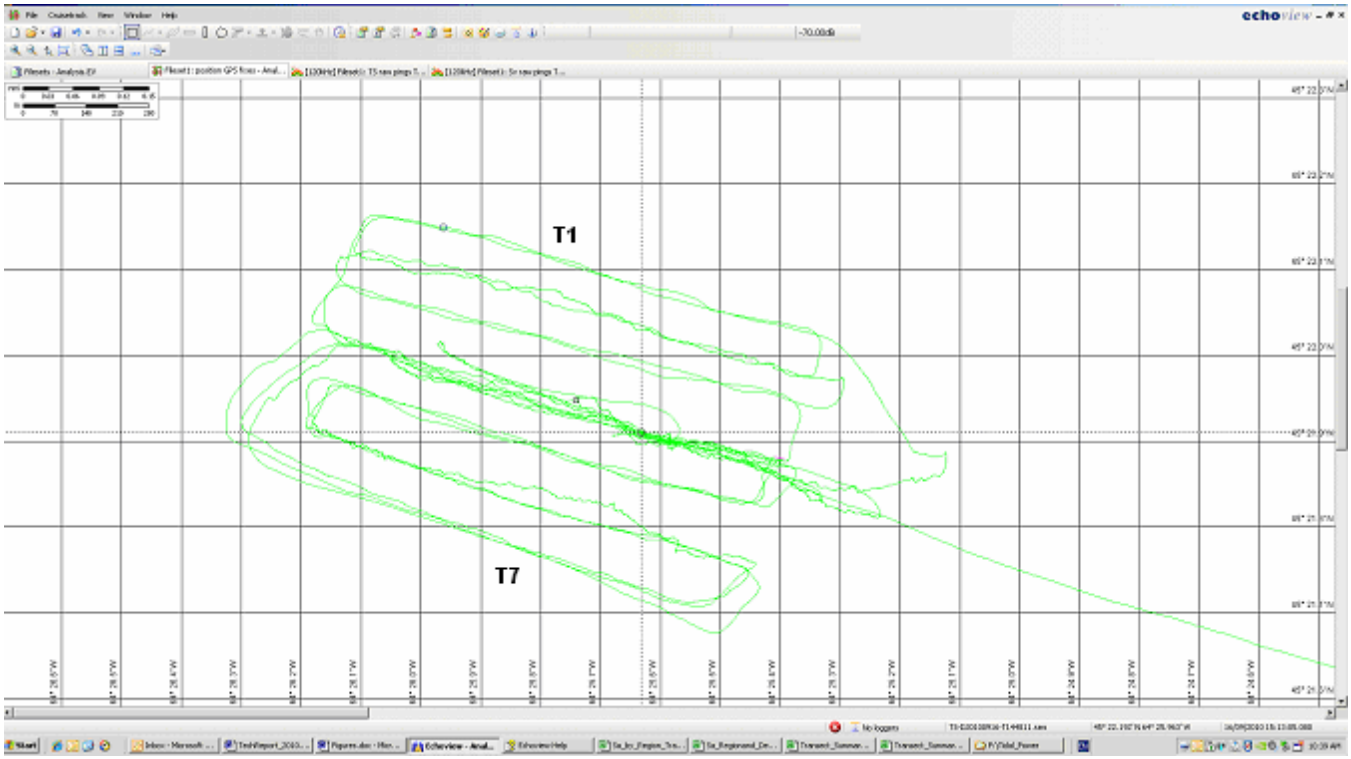

Figure 6. Vessel track and transects for the survey conducted on 16 Sept. 2010 in Minas Channel. Note transects are numbered from north to south as 1 to 7 with transect 4 including the turbine (designated by cross hairs).

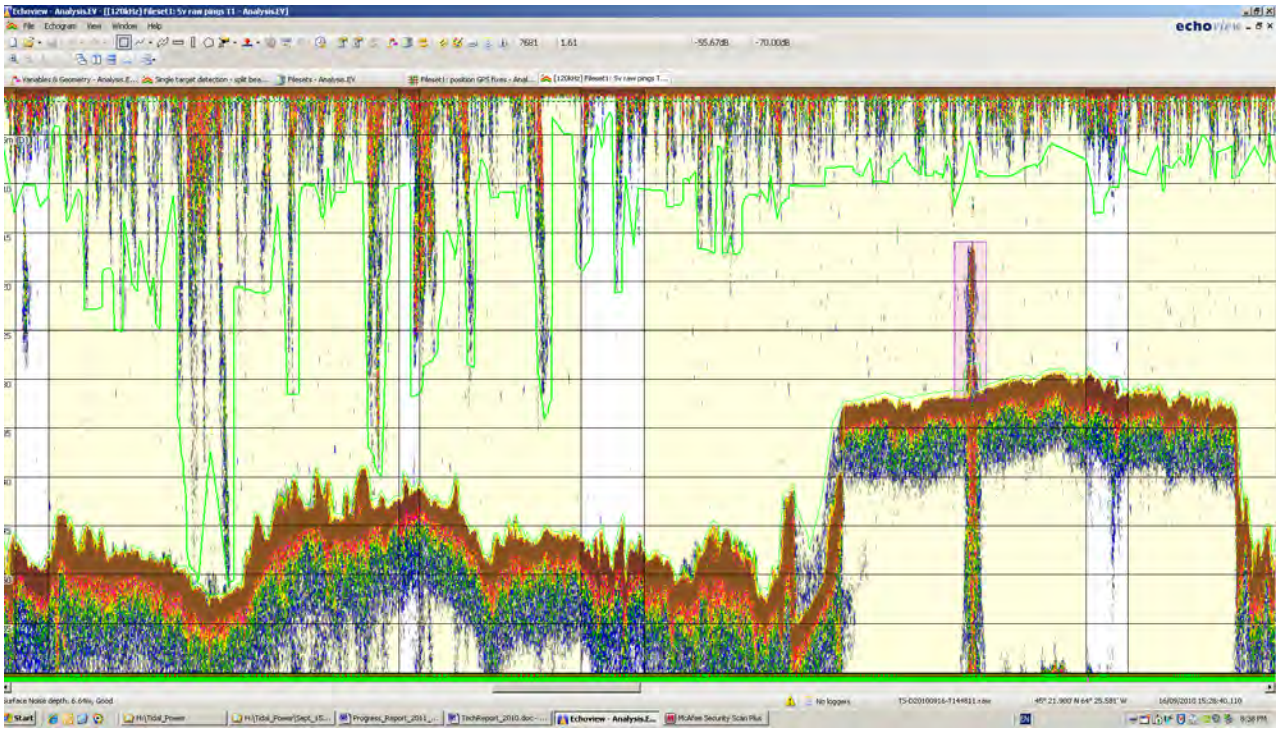

Figure 7. EK60 echogram illustrating the surface, surface noise, and bottom boundaries (green). The yellow shading defines the transects and the pink shading the area associated with the turbine.

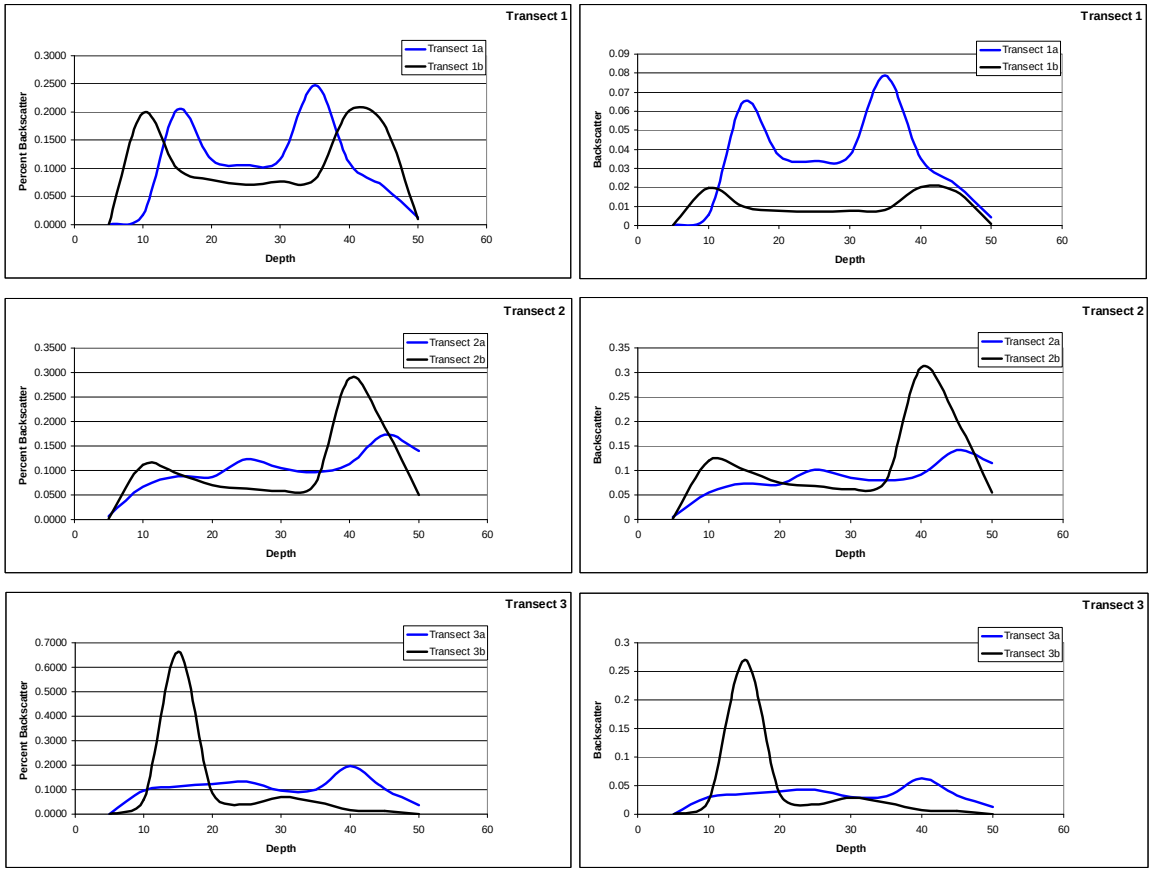

Figure 8. Summary of backscatter (NASC) by 5 m depth intervals as a portion of the total (left) and the absolute (right) for transects 1-3 located north of the turbine.

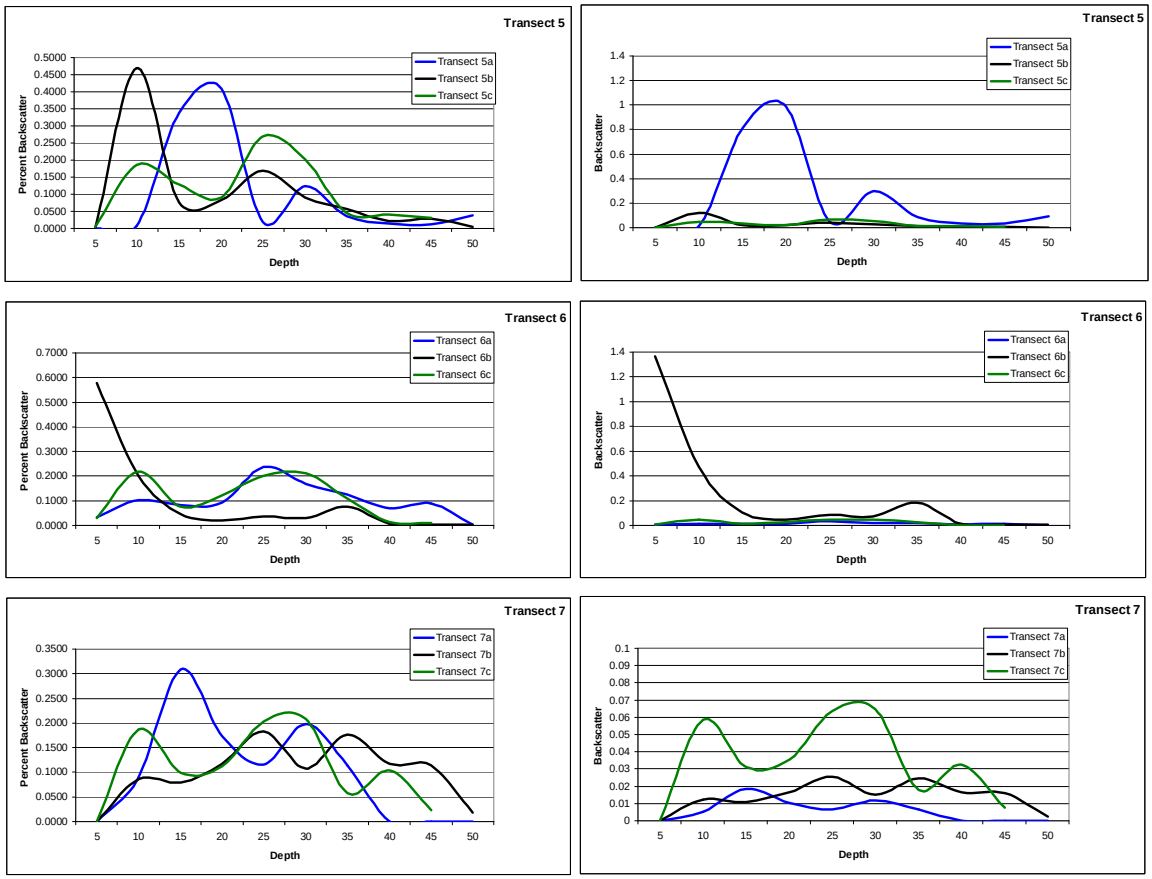

Figure 9. Summary of backscatter (NASC) by 5m depth intervals as a portion of the total (left) and the absolute (right) for transects 5-7 located south of the turbine.

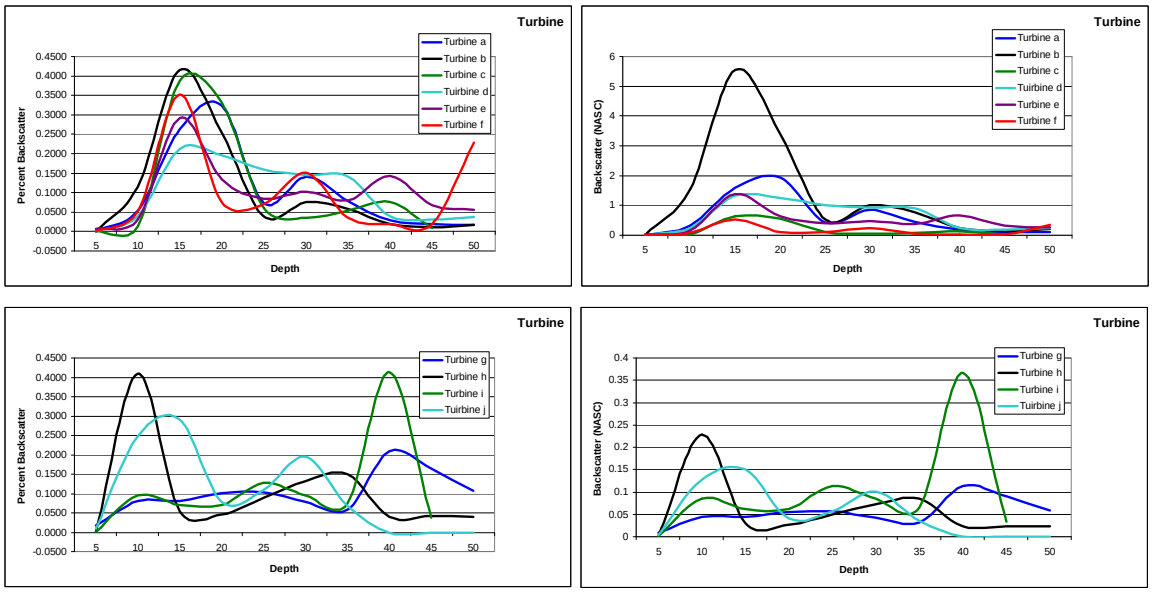

Figure 10. Summary of backscatter (NASC) by 5m depth intervals as a portion of the total (left) and the absolute (right) for all transects over the turbine (Transect 4).

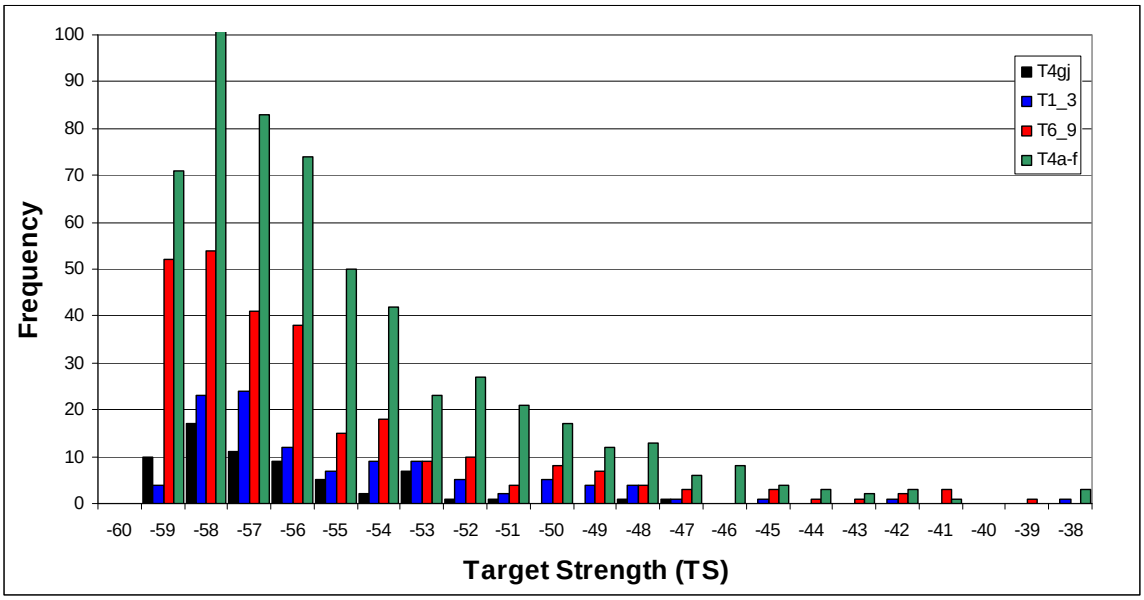

Figure 11. Target strength distribution for all four areas. See text for explanation.

Figure 12. Scatter plots of TS by depth for selected transects combined.

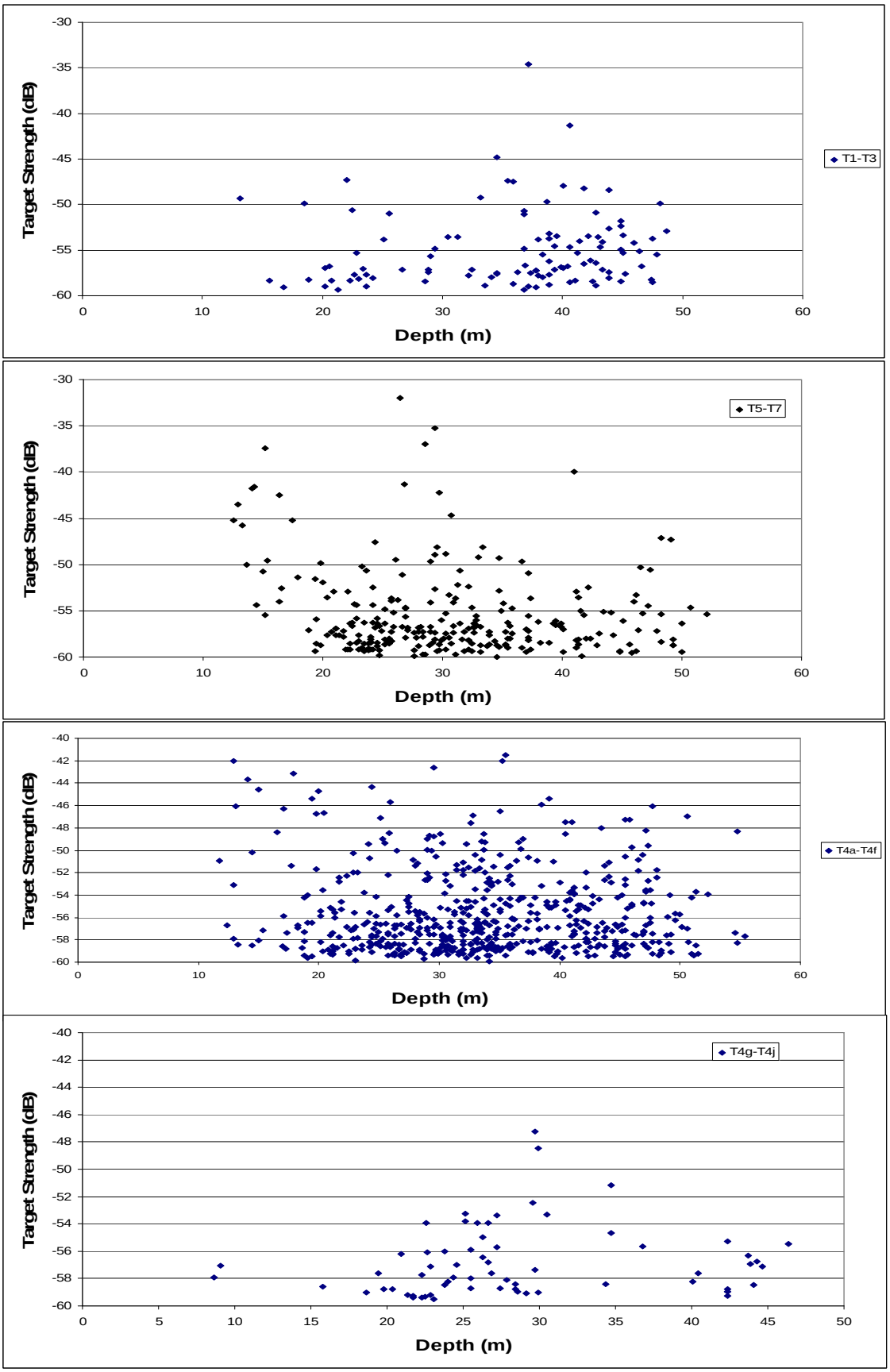

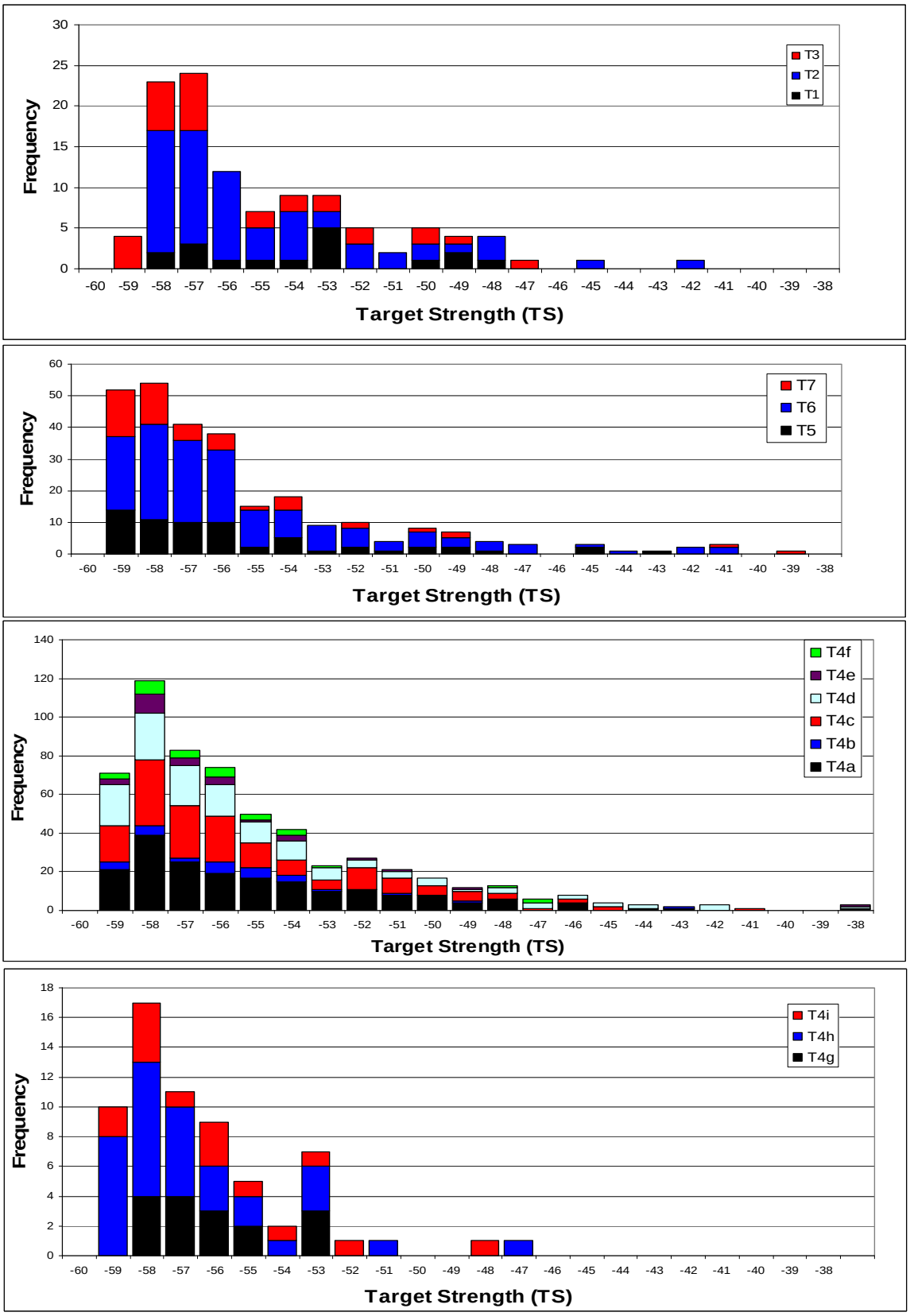

Figure 13. Target strength distribution by transects for all individual runs.

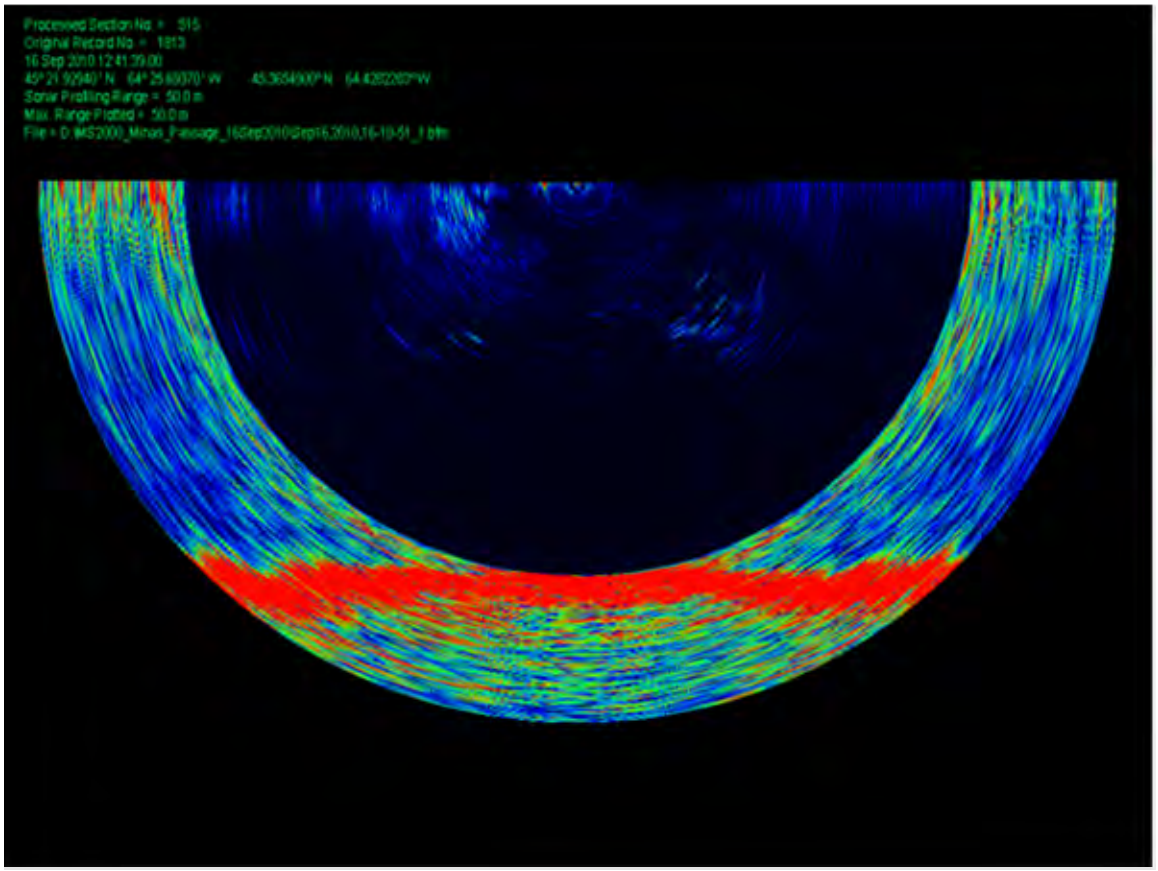

Figure 14. Simrad MS 2000 multi-beam 2-D fan section. Range to outer edge of coloured semicircle is 50 m. The horizontal red horizon is the bottom at a depth of 36 m. Intense scattering off the bottom interferes with all synthesized beams limiting the maximum effective water column profiling range to the distance from transducer to the nearest point on bottom. Around 15 m depth a heterogeneous layer of fish can be observed. Above the fish can be seen water column scattering of bubble cloud origin.

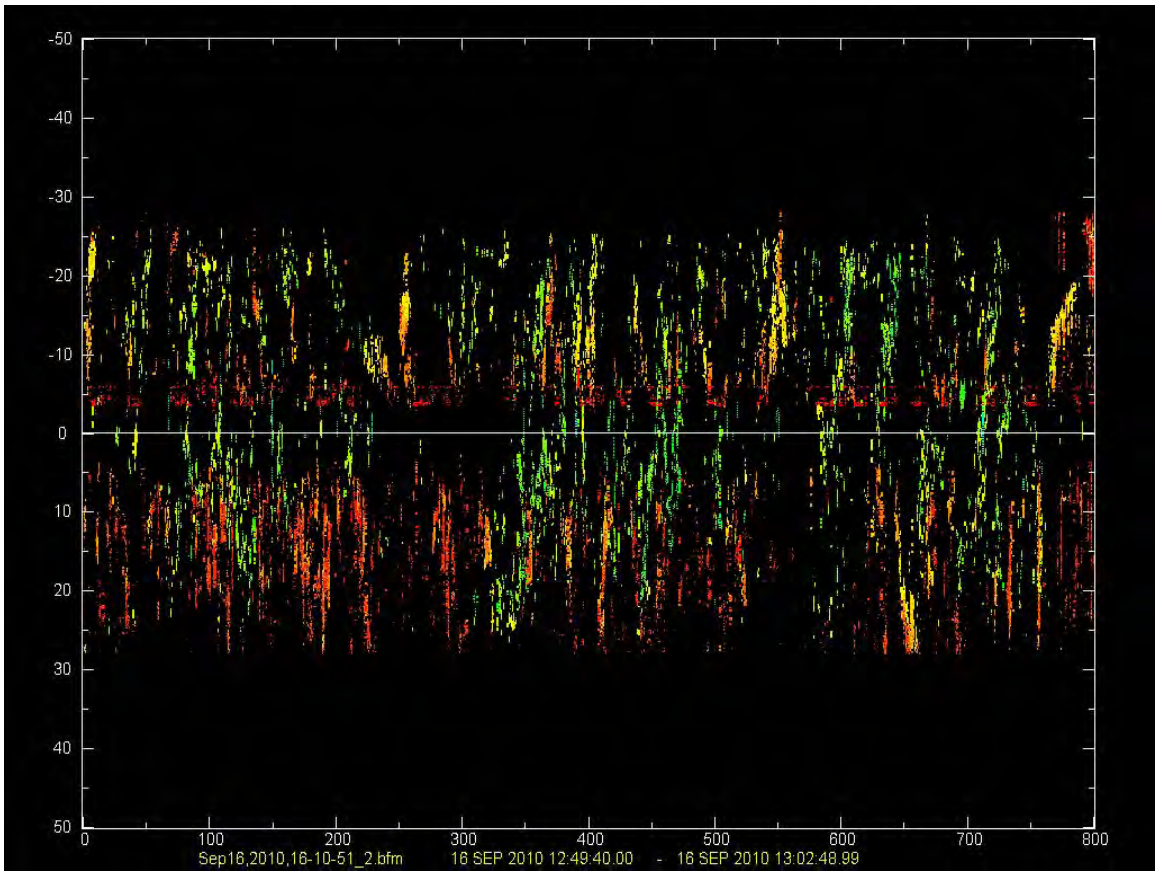

Figure 15. Aerial view of observed Simrad MS 2000 multi-beam field of view, looking downwards, over pings 1 to 800 of beamformed file Sept16,2010,16-10-51_2.bfm. Data series extends from 12:49:40 to 13:02:49 GMT, 16 Sept. 2010. This recording was conducted while the vessel steamed a loop just east of the turbine when shallow fish targets were especially numerous on the strong ebb tide cycle. Data is reproduced out to a maximum radial range of 28 m from the transducer. Negative to positive Y axis values correspond to Port and Starboard distances respectively from the transducer in meters. The X axis shows ping number. Depth is colour-encoded, ranging from red at surface to blue at depth. Shallow bubble clouds show up as shades of red to yellow while fish near 15 m depth appear in green. A few deeper fish targets or acoustic artefacts show up as blue.

(A)

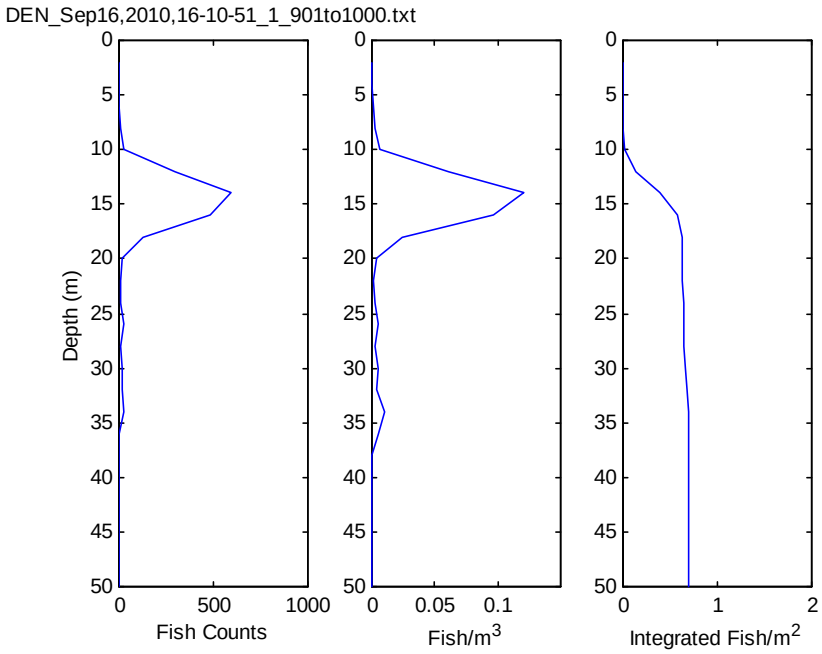

(B)

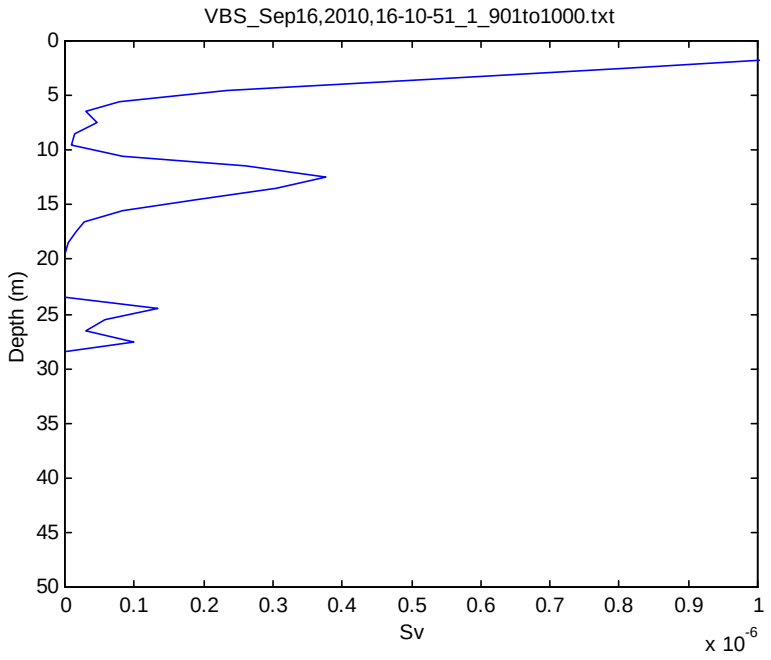

Figure 16. Comparison of fish density vs. depth (A) and volume backscattering strength component vs. depth (B) for an identical 100 ping section extending from ping 901 to ping 1000 of beamformed file: Sep16,2010,16-10-51_1.bfm. Data shown was gathered immediately east of turbine between 12:48:01 and 12:49:39 GMT on the strong portion of the ebb tide cycle.

(A)

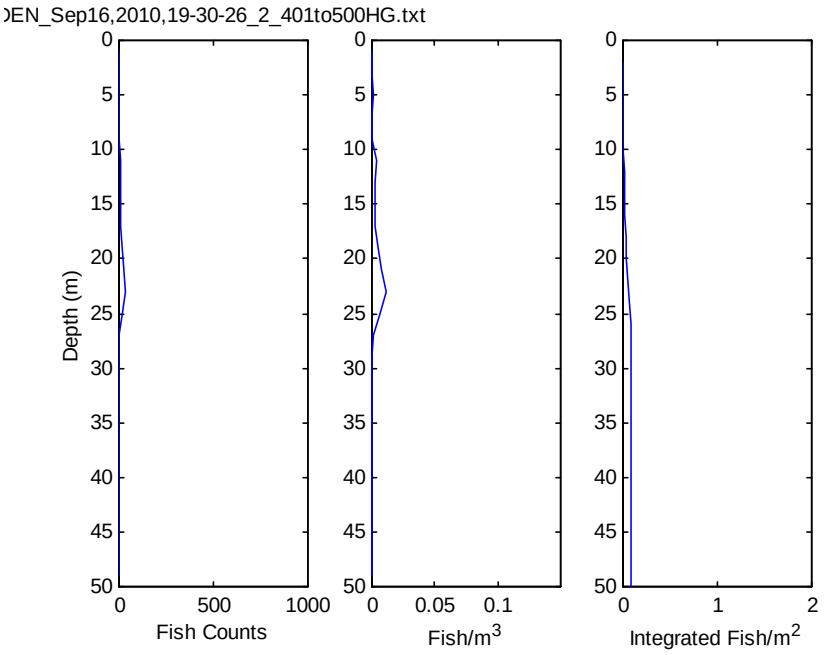

(B)

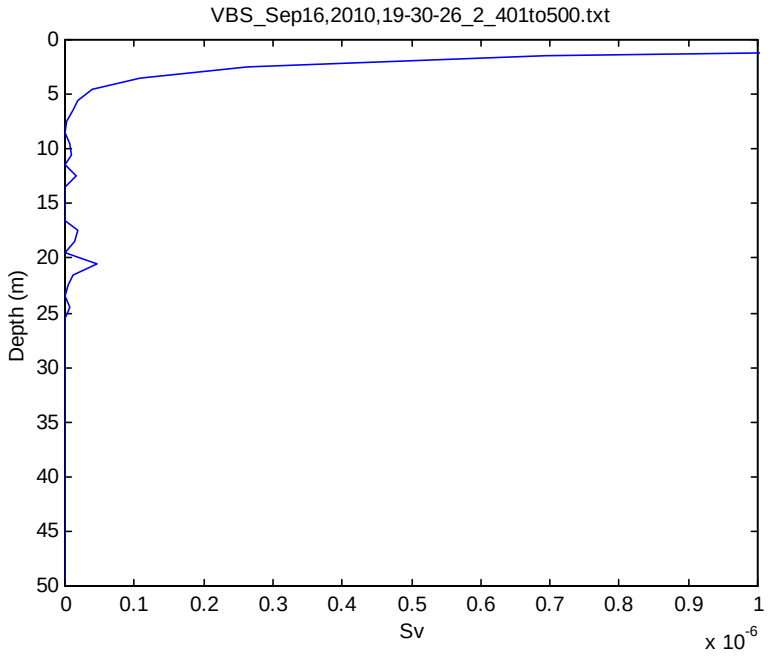

Figure 17. Comparison of fish density vs. depth (A) and volume backscattering strength component vs. depth (B) for an identical 100 ping section extending from ping 401 to ping 500 of beamformed file: Sep16,2010,19-30-26_2.bfm. Data shown was gathered immediately east of turbine between 16:15:31 and 16:17:09 GMT near the end of the ebb current cycle.

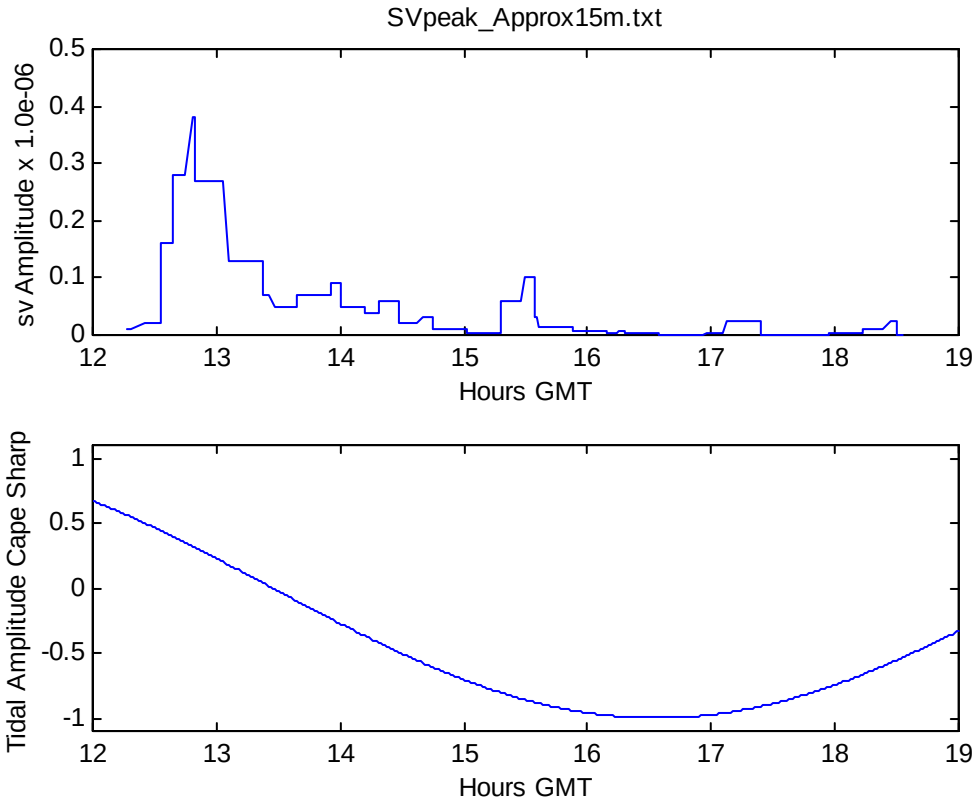

Figure 18. (Top) Peak S_v amplitude (scaling arbitrary) of ~15 m depth layer vs. time. (Bottom) Sinusoidal approximation to tidal amplitude. Plotted observation period extends from 12:16:43 to 18:33:10 GMT.

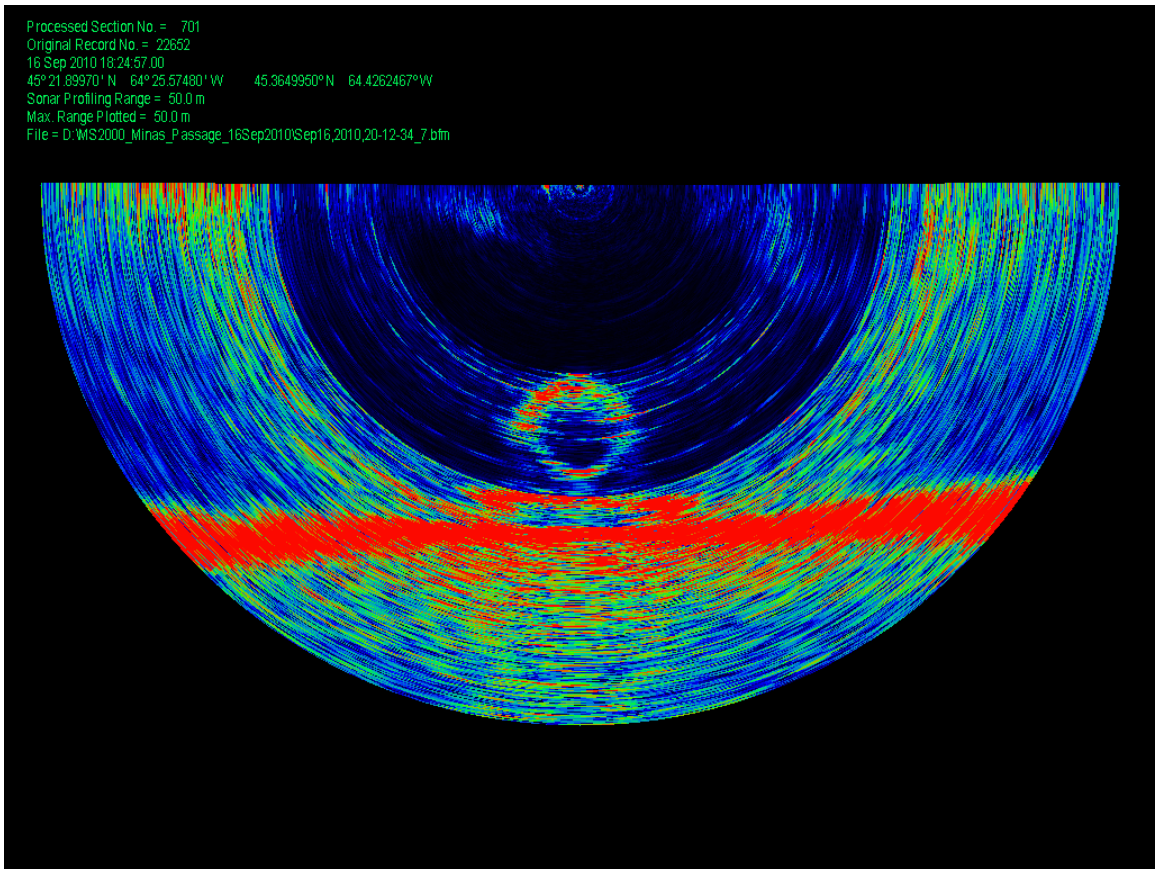

Figure 19. Simrad MS 2000 section showing Open Hydro turbine and its base. Note interference in all synthesized beams from intense backscatter originating from the turbine structure.

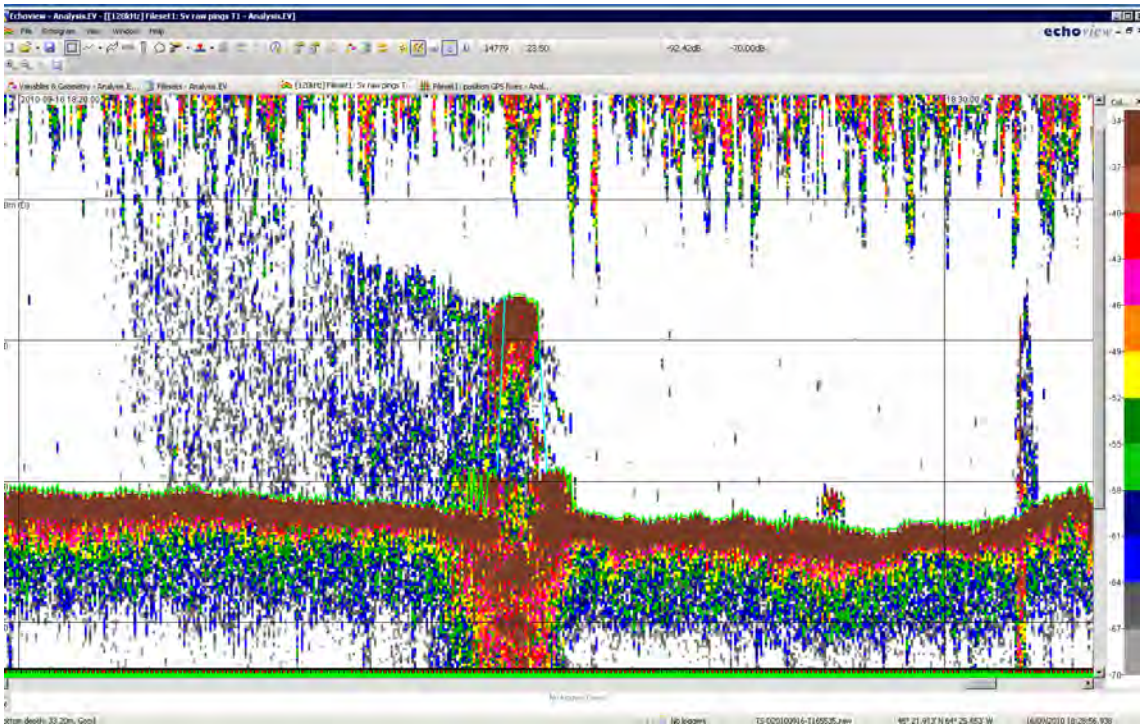

Figure 20. EK60 echogram showing an acoustically visible wake apparently ascending to the surface on transect over turbine (near center). Bubble clouds can also be observed extending down from surface. Vessel was moving slowly east to west against the flood tide.

APPENDIX I: COMPUTATION OF OBSERVED WATER VOLUME IN MULTI-BEAM FAN SECTION

THEORY

Assume an (X, Y, Z) coordinate system X +ve to the right, Y +ve out of the page, and Z +ve downward. Let the origin (0, 0, 0) be the position of the sonar transducer with the fan in the plane of the page, and symmetrical about the Z axis (Fig. A1(A)).

Let R_{Max} be the maximum effective sonar radial range (e.g. 50 m). In deep clear water this distance will normally correspond to the maximum sonar 1-way range setting. If a very strong scatterer, such as the ocean bottom or the turbine structure lies within the sonar range setting, its minimum radial range from the transducer usually determines the maximum effective observations range for fish targets since reflected energy from this scatterer enters the side lobes of all synthesized fan beams often introducing non-linearities into the beam forming process. This normally obscures all fish targets at still greater ranges and therefore defines a maximum effective observation or viewing range equal to the minimum transducer to scatterer distance.

For the process of manual fish counting and of computing a fish density over a defined depth interval, namely depths z_1 to z_2, it is necessary to compute the water volume, V, observed between the upper and lower bounding depths out to a radial range R_{Max} on a 180^0 fan beam echogram (i.e. contiguous or overlapping beams cover the entire section from -90^0 to $+90^0$ from the vertical.

To proceed: At vertical range z from the transducer let a horizontal strip be extracted from the observed fan water volume for 1 sonar transmission or "ping", the strip running horizontally through the receiving fan (Fig. A1(B)). The out-of-fan, i.e. (X, Y) plane, half-width of this strip as a function of $y(x)$, when θ is small, is given to a very good approximation by:
$y = R\sin\theta$ where θ is the "effective", and everywhere constant, half-beamwidth of the semi-cylindrical Mills Cross radiating element out of the (X, Z) plane. This approximation ignores the very slight curvatures of this strip for individual fan beams comprising this strip for a given sonar travel-time range.

The receiving array beamwidth is much larger than the transmit beamwidth in the same plane and, therefore, has little influence on the combined transmit-receive response. Let A be the total area of the observed horizontal strip:

$$V = \int_{z_1}^{z_2} A(z).dz \qquad (1)$$

where

$$A(z) = 4\int_{0}^{x_{Max}} y(x).dx$$

$$= 4\int_{0}^{X_{Max}} \sqrt{x^2 + z^2}.\sin\theta.dx \qquad (2)$$

$$= 2\sin\theta \left| x\sqrt{x^2 + z^2} + z^2 \log\left(x + \sqrt{x^2 + z^2}\right)\right|_{0}^{X_{Max}}$$

$$= 2\sin\theta\left[X_{Max}\sqrt{X_{Max}^2 + z^2} + z^2 \log\left(X_{Max} + \sqrt{X_{Max}^2 + z^2}\right) - z^2 \log z\right]$$

For a given R_{Max}, X_{Max} is a function of z:

$$A(z) = 2\sin\theta\left[\sqrt{R_{Max}^2 - z^2}\ R_{Max} + z^2 \log\left((\sqrt{R_{Max}^2 - z^2} + R_{Max}\right) - z^2 \log z\right] \qquad (3)$$

The observed volume can be found by substituting $A(z)$ from equation (3) into (1). This yields an integral that cannot be evaluated in closed form but which can be readily approximated numerically by a finite sum using a reasonably small incremental Δz between the limits z_1 and z_2.

IMPLEMENTATION

In implementation, for the 16 Sept. 2010 Minas Passage data set, fish density is estimated in contiguous 2 m vertical bins. To compute the finite sum approximating the integral of Equation (1) a Δz of 0.2 m is employed.

A critical question is the selection of the "effective" half-beamwidth θ. For the initial reduction of the Minas Passage data to fish density, a unit "effective" beamwidth of 1^0 or a half-beamwidth of 0.5^0 was assumed. The manufacturer's stated nominal -3 dB to -3 dB beamwidth of the MS 2000 linear transmit array used in Mills Cross configuration with the receive array is 1.5^0. Assigning a realistic half-beamwidth reduces to determining the maximum angular displacement from the central fan plane that a fish can be located and still be identified as a valid fish target on manual inspection of the fan section echogram. Clearly, this depends on the signal-to-noise ratio of the fish target echo if it were fan-centered which, in turn, is dependent on its target strength, observation, range and a number of instrumentation and environmental parameters. Therefore, the "effective" beamwidth might be expected to vary somewhat with the nature of the target and with the target observation range.

An approximate estimate of the dynamic range from strongest observed echoes to minimum detectable echoes during the manual counting process is about 20 dB – perhaps slightly more. The -20 dB point for a shaded line array transmit element should occur at an off-axis angle about 2.5 times the -3 dB off-axis angle (see measurements for 90 kHz SM2000 with nominal 1.5^0 transmit beam in Foote et al. (2005), and typical shaded line array responses shown in Clay & Medwin (1977). Therefore, for counting stronger fish targets the effective detection beamwidth of the transducer actually utilized should be in

the neighbourhood of 2.5 x 1.5^0 ~ 3.75^0 yielding an effective half-beamwidth of just under 2^0. Consequently, the fish densities computed with a reference 1^0 beam should be decreased by a factor of about 3.75 to give the best estimate of the actual physical fish density.

It should be noted that estimates based on manual counting are at to a degree "hand-waving" and in most instances should in no way be interpreted as definitively as those furnished by a split-beam quantitative fisheries echosounder like the Simrad EK60. The principal reason for considering multi-beam derived fish densities is the comparatively large observed water column volume afforded by the multi-beam fan as compared to a typical split-beam water volume, important when targets are sparse. Manual selection of multi-beam targets also affords a high degree of spurious bubble cloud echo rejection.

REFERENCES (APPENDIX)

Clay, C. S. and Medwin, H. 1977. Acoustical Oceanography: Principles and Applications. John Wiley & Sons, New York. 544 pp.

Foote, K. G., Chu, D., Hammar, T. R., Baldwin, K. C., Mayer, L. A., Hulfnagle, Jr., L. C., and Jech, J. M. 2005. Protocols for calibrating multibeam sonar. J. Acoust. Soc. Am. 117(4), Pt. 1: 2013 – 2027.

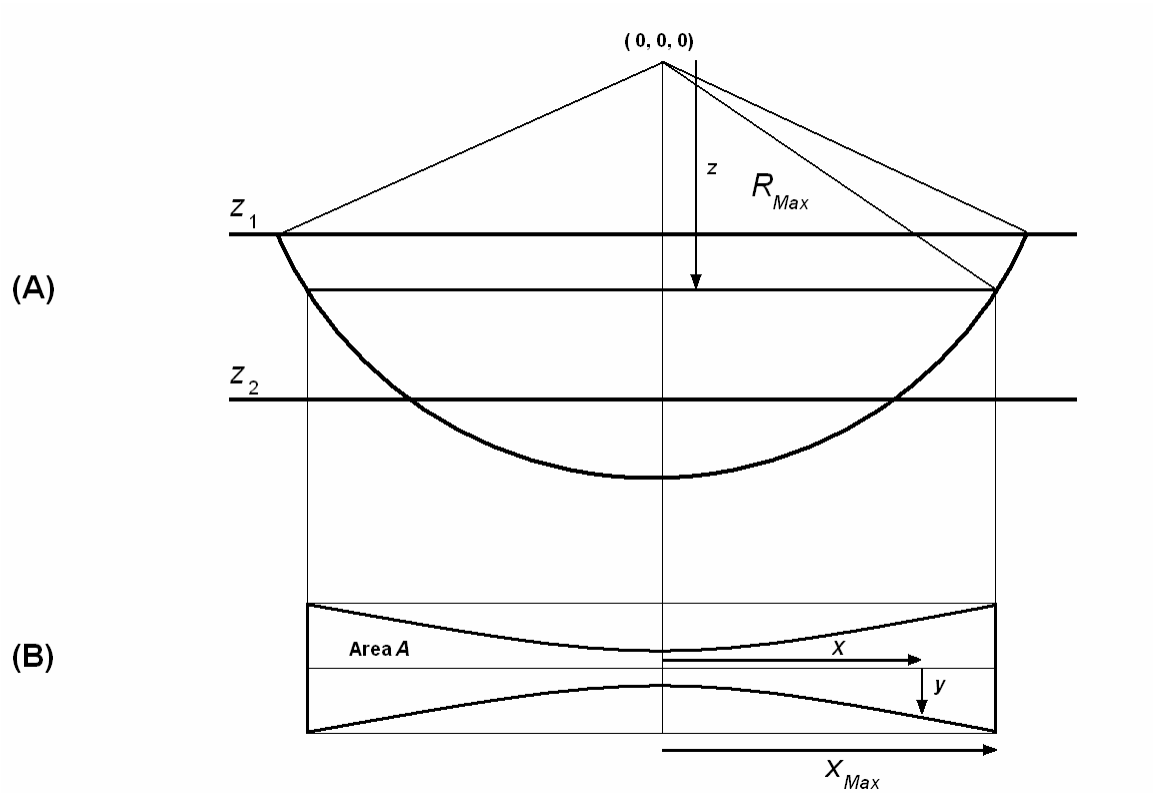

Figure A1. Sonar observation geometry. (A) – Observed volume in (*X*, *Z*) plane between depths z_1 and z_2 and extending radially from the transducer origin (0, 0, 0) to maximum viewed radial range R_{Max} from the transducer.(B) – Observed strip in (*X*, *Y*) plane at depth *z*.